National Library of Canada
Bibliothèque nationale du Canada

Canadian Theses Service
Services des thèses canadiennes

Ottawa, Canada
K1A 0N4

CANADIAN THESES

THÈSES CANADIENNES

NOTICE

The quality of this microfiche is heavily dependent upon the quality of the original thesis submitted for microfilming. Every effort has been made to ensure the highest quality of reproduction possible.

If pages are missing, contact the university which granted the degree.

Some pages may have indistinct print especially if the original pages were typed with a poor typewriter ribbon or if the university sent us an inferior photocopy.

Previously copyrighted materials (journal articles, published tests, etc.) are not filmed.

Reproduction in full or in part of this film is governed by the Canadian Copyright Act, R.S.C. 1970, c. C-30.

AVIS

La qualité de cette microfiche dépend grandement de la qualité de la thèse soumise au microfilmage. Nous avons tout fait pour assurer une qualité supérieure de reproduction.

S'il manque des pages, veuillez communiquer avec l'université qui a conféré le grade.

La qualité d'impression de certaines pages peut laisser à désirer, surtout si les pages originales ont été dactylographiées à l'aide d'un ruban usé ou si l'université nous a fait parvenir une photocopie de qualité inférieure.

Les documents qui font déjà l'objet d'un droit d'auteur (articles de revue, examens publiés, etc.) ne sont pas microfilmés.

La reproduction, même partielle, de ce microfilm est soumise à la Loi canadienne sur le droit d'auteur, SRC 1970, c. C-30.

THIS DISSERTATION HAS BEEN MICROFILMED EXACTLY AS RECEIVED

LA THÈSE A ÉTÉ MICROFILMÉE TELLE QUE NOUS L'AVONS REÇUE

NL-339 (r.86/06)

Canada

THE UNIVERSITY OF ALBERTA

FABMS - A MECHANISTIC STUDY

BY

CUMERASIRI RAWEENDRA KULATUNGA

A THESIS

SUBMITTED TO THE FACULTY OF GRADUATE STUDIES AND RESEARCH IN PARTIAL FULFILMENT OF THE REQUIREMENTS FOR THE DEGREE OF MASTER OF SCIENCE

DEPARTMENT OF CHEMISTRY

EDMONTON, ALBERTA

FALL 1986

Permission has been granted to the National Library of Canada to microfilm this thesis and to lend or sell copies of the film.

The author (copyright owner) has reserved other publication rights, and neither the thesis nor extensive extracts from it may be printed or otherwise reproduced without his/her written permission.

L'autorisation a été accordée à la Bibliothèque nationale du Canada de microfilmer cette thèse et de prêter ou de vendre des exemplaires du film.

L'auteur (titulaire du droit d'auteur) se réserve les autres droits de publication; ni la thèse ni de longs extraits de celle-ci ne doivent être imprimés ou autrement reproduits sans son autorisation écrite.

ISBN 0-315-32322-1

THE UNIVERSITY OF ALBERTA

RELEASE FORM

NAME OF AUTHOR: CUMERASIRI RAWEENDRA KULATUNGA

TITLE OF THESIS: FABMS - A MECHANISTIC STUDY

DEGREE: MASTER OF SCIENCE

YEAR THIS DEGREE GRANTED: FALL 1986

PERMISSION IS HEREBY GRANTED TO THE UNIVERSITY OF ALBERTA LIBRARY TO REPRODUCE SINGLE COPIES OF THIS THESIS AND TO LEND OR SELL SUCH COPIES FOR PRIVATE, SCHOLARLY OR SCIENTIFIC RESEARCH PURPOSES ONLY.

THE AUTHOR RESERVES OTHER PUBLICATION RIGHTS, AND NEITHER THE THESIS NOR EXTENSIVE EXTRACTS FROM IT MAY BE PRINTED OR OTHERWISE REPRODUCED WITHOUT THE AUTHOR'S WRITTEN PERMISSION.

C. R. Kulatunga

(STUDENT'S SIGNATURE)

(STUDENT'S PERMANENT ADDRESS)

10, Dakshinarama Road,
Mount Lavinia
Sri Lanka

THE UNIVERSITY OF ALBERTA

FACULTY OF GRADUATE STUDIES AND RESEARCH

THE UNDERSIGNED CERTIFY THAT THEY HAVE READ, AND RECOMMENDED TO THE FACULTY OF GRADUATE STUDIES AND RESEARCH FOR ACCEPTANCE, A THESIS ENTITLED "FABMS - A MECHANISTIC STUDY", SUBMITTED BY CUMERASIRI RAWEENDRA KULATUNGA IN PARTIAL FULFILMENT OF THE REQUIREMENTS FOR THE DEGREE OF MASTER OF SCIENCE.

P. Kelly
.....
(SUPERVISOR)
.....
Byron Kratochvil
.....
Jerry A. Plewchuk
.....
T. J. Coutts
.....

DATE: 17-6-86

ABSTRACT

Fast Atom Bombardment (FAB) spectra of neutral binary solutions consisting of compounds with a wide range of gas phase basicities were obtained. The major ions observed were MH^+, LH^+, M_2H^+, L_2H^+ and the mixed cluster ions $M_xL_yH^+$ where M = analyte and L = matrix. In most cases the spectrum of the component with the lower gas phase basicity was suppressed. The compounds chosen are frequently used as FAB matrices, and they are in the order of decreasing gas phase basicity: triethanolamine (TEA), diethanolamine (DEA), 4 - octylaniline, 1, 2, 4 - butanetriol, glycerol (Gly) and 3 - nitrobenzyl alcohol (NOBA). The gas phase basicities and proton affinities (P.A.) of these compounds were determined in this laboratory in separate experiments by J. Sunner using a high pressure ion source mass spectrometer.

The positive total ion currents (TIC) emitted during FAB of glycerol (matrix) solutions of alkali chlorides, HCl, and pyridinium hydrochlorides (analytes) were measured as a function of the concentration of the electrolytes. Although the intensities of the major ions of the matrix and of the analytes changed significantly upon the addition

of salts, TIC remained relatively constant. The author is of the opinion that the above experimental results are compatible with a Gas Collision Model (G.C.M.) which has the following main characteristics. Ions formed in the liquid sample due to the atom impact undergo extensive recombination reactions. This occurs in a cavity filled with a high temperature, high density gas, formed as a result of the incident fast atoms. During the expulsion of the "hot gas" into the vacuum, ion molecule reactions will occur between various ionic molecules, fragments and neutral molecules, which will lead to the formation of pseudomolecular ions, cluster ions and fragment ions.

ACKNOWLEDGEMENTS

I wish to express my sincere appreciation to Dr. Paul Kebarle, for his invaluable guidance and support throughout the course of this work.

I would like to thank Dr. J. Sunner for his help on certain aspects of this work. His interest and helpful discussions are truly appreciated. Thanks are also extended to Dr. A. Hogg and to the staff of the mass spectrometry laboratory for their assistance with this project.

Finally, I am extremely grateful to my parents and thank them for their assistance and sacrifices that they have made for many years on my behalf.

TABLE OF CONTENTS

	Page
Abstract	iv
Acknowledgements	vi
List of Tables	xi
List of Figures	xiii
1.0 INTRODUCTION	
1.1 The origin and development of FABMS . .	1
1.2 Neutral atom beams employed in FABMS . .	4
1.3 The influence of the angle of incidence on intensity	5
1.4 Role of the matrix in FABMS analysis . .	6
1.4.1 Solubility	7
1.4.2 Volatility	7
1.4.3 Viscosity	8
1.4.4 Basicity	8
1.5 Commonly used matrices for FAB	11
1.5.1 Glycerol	11
1.5.2 Thioglycerol	12
1.5.3 Meta-nitrobehzyl alcohol	12
1.5.4 Diethanolamine and triethanolamine	13

Page

1.6 Sensitivity enhancement by matrix modification 13

2.0 IONIZATION MODELS FOR FABMS

2.1.1 Precursor model - SIMS of solids 16

2.1.2 Precursor model - preformed ions in liquid matrices 17

2.2 Desorption ionization model 18

2.3 Gas phase collision model 20

3.0 EXPERIMENTAL

3.1 General description 23

3.2 Fast atom bombardment gun 24

3.3 Ion source 26

3.4 Analyzer 27

3.4.1 Electrostatic analyzer 27

3.4.2 Magnetic analyzer 28

3.5 Detection of ions 29

3.6 Experimental conditions, procedures and reagents 30

Page

4.0 RESULTS AND DISCUSSION

4.1 Verification of the role of proton affinity in FABMS 32

4.2 Preference factors 41

4.3 The relevance of the precursor model and the G.C.M. in FABMS 44

4.4 Stability of protonated dimers and their intensities in FABMS 48

5.0 SECONDARY ION CURRENTS IN FABMS OF PREIONIZED LIQUIDS IN FAB

5.1 The influence of alkali chlorides on FAB spectra 55

5.2 The influence of HCl on FAB spectra . . 70

5.3 Total ion currents in the gas collision model 82

5.4 Evidence for recombination reactions . . 83

5.4.1 Estimate of ions produced per FAB particle 83

5.4.2 Ions from liquid matrix and analyte 85

Page

5.5 Thermodynamic feasibility of analyte ion formation from ion pairs 88

5.6 Preference factors of alkali chloride solutions 90

6.0 CONCLUSION 94

REFERENCES 96

LIST OF TABLES

Table		Page
(1)	Summary of FAB spectra of 10% (mole) binary mixtures	34
(2)	Stabilities of proton bound matrix dimers	50
(3)	Total ion currents of alkali chlorides in glycerol	52
(4)	FABMS peak intensities of alkali chlorides	59
(5)	Fragment to monomer intensity ratios of glycerol in KCl/glycerol solutions . . .	61
(6)	Dimer to monomer intensity ratios of glycerol in KCl/glycerol solutions . . .	63
(7)	Preference factors of K^+ over glycerol and in TEA	66
(8)	Preference factors of alkali ions in glycerol and in TEA	68
(9)	Total ion currents of Gly/HCl solutions .	71
(10a)	Intensities of the main glycerol ions in HCl/Gly solutions	73
(10b)	Intensities of the $GlyH^+$ in Gly/HCl solutions	73

Table		Page

(11) Intensity ratios of the main fragments of glycerol to the intensity of $GlyH^+$ 75

(12) Intensity ratios of dimer to monomer peaks of glycerol in HCl/Gly solutions . . 75

(13) Variation of TIC of DEA HCl/DEA solutions . 79

(14) Correlation between intensity ratio of $M^+(Gly)/M^+$ and $-\Delta G°_{16}$ 90

LIST OF FIGURES

Figure		Page
(1)	Ejection of secondary ions in the precursor model	16
(2)	Nier-Johnson double focussing mass analyzer	23
(3)	Schematic diagram of FAB gun showing internal structure	24
(4)	FAB ion source	26
(5)	FAB spectrum of TEA in NOBA	36
(6)	FAB spectrum of glycerol in TEA	37
(7)	FAB spectrum of glycerol in octyl-aniline	38
(8a)	FAB spectrum of neat TEA	43
(8b)	FAB spectrum of TEA in NOBA	43
(9a)	Chemical ionization mass spectrum of glycerol in 4 torr of methane with 2% (mole) benzene	47
(9b)	Chemical ionization mass spectrum of glycerol in 4 torr of methane	47
(9c)	FAB spectrum of neat glycerol	47

Figure		Page

(10) TIC from glycerol solutions of alkali chlorides 54

(11) FAB spectrum of LiCl in glycerol 56

(12) FAB spectrum of NaCl in glycerol 57

(13) FAB spectrum of KCl in glycerol 58

(14) Sum of intensities of all K^+ containing ions, sum of intensities of the main glycerol ions and sum of intensities of background ions 60

(15) Ratio of sum of intensities of the main glycerol fragments 75^+, 57^+ and 45^+ to the intensity of the protonated glycerol ions 62

(16) Ratio of protonated glycerol dimer to the protonated monomer 64

(17) Preference factors for K^+ containing ions over the main glycerol ions 67

(18) Preference factors for alkali containing ions over matrix ions for 1 mole percent solutions of alkali chlorides in glycerol and in triethanolamine 69

Figure		Page

(19) TIC of glycerol with concentrated HCl and TIC for glycerol with pyridinium hydrochloride 72

(20) Sum of intensities of main glycerol ions and intensities of protonated glycerol ions 74

(21) Ratio of sum of intensities of the main glycerol fragments, 75^+, 57^+ and 45^+, to the intensity of the protonated glycerol ions 76

(22) Ratio of the protonated glycerol dimer to the protonated monomer 78

(23) TIC for mixtures of diethanolamine and diethanolamine hydrochlorides 80

(24) Energy stability diagram of NaCl in the gas phase 84

(25) Correlation between the FAB intensity ratio at 1 mole percent MCl: $M^+(Gly)/M^+$ and $-\Delta G°_{16}$ at 300 K for the clustering reaction $M^+ + 2\ H_2O \longrightarrow M^+(H_2O)_2$ for $M^+ = Li^+$, Na^+, K^+ and Rb^+ 91

CHAPTER I

INTRODUCTION

1.1 The origin and development of FABMS

Fast Atom Bombardment Mass Spectrometry (FABMS) was first introduced by Michael Barber in 1981 (1). A significant advantage of this method compared to other routine mass spectrometric methods is that the sample need not be thermally vapourized before it is ionized. Thus, FABMS is a method of obtaining mass spectra of substances which are nonvolatile and unstable at the temperatures required to evaporate them. FABMS has therefore been used with considerable success on substances of biological and biomedical importance. These substances are mostly non-volatile due to their high molecular weights and high polarity.

In FABMS, the analyte (M) is first dissolved in a suitable liquid matrix (L). The sample is then spread uniformly on the flat tip of a metal rod, which is fixed to a sample insertion probe. The probe, which is used to introduce the sample into the ion source, is placed near the ion exit slit of a conventional mass spectrometer ion source. The sample is bombarded by a beam of fast atoms,

usually xenon or argon. The secondary ions produced by the bombardment are then mass analyzed.

A cold cathode discharge ion source is normally employed as the source of fast atoms in FABMS. The discharge produces a beam of ions of the neutral gas. Some of these ions collide with the neutral atoms of the same gas. As a result of the collisions of the accelerated ions with the atoms, a charge exchange takes place with little change in forward momentum as follows:

$$\underset{\text{fast ions}}{A^+} + A \longrightarrow \underset{\text{fast atoms}}{A} + A^+ \quad (1)$$

The resulting fast atoms have energies in the 2-8 keV range, depending on the discharge voltage used (2). In most cases the ionic component is cleansed from the fast atom beam by a set of electrostatic deflection plates.

The major category of ions observed by the bombardment of the sample M contained in the matrix L are the so called "pseudomolecular" ions MH^+, LH^+ in the positive ion spectra and $(M-H)^-$, $(L-H)^-$ in the negative ion spectra. A second category of observed ions are charged fragments of both the analyte and the matrix. The third class are cluster ions M_xH^+ and L_yH^+ and mixed clusters $M_xL_yH^+$. These are composed of analyte and matrix molecules and one proton.

The FABMS method is similar to Secondary Ion Mass Spectrometry (SIMS). SIMS has been used since the mid-1970's. Samples, usually in the solid form, are bombarded with ions of kilo-electron-volt energy. The positively and negatively charged secondary ions emanating from the sample are then mass analyzed.

It was noted by Vickerman and Barber (3) that, when insulating samples were bombarded by ions, a potential of about 3-5 kV was induced on the samples. This potential deflected the incident ion beam. To overcome this problem they used fast atoms to bombard the samples. They then observed that the period of time during which they were able to detect the secondary ions was very short. Next they dissolved the analytes in a liquid matrix, glycerol, prior to the bombardment, and observed that a liquid matrix increases the duration of the secondary ion emission considerably.

Cooks (4) and Benninghoven (5) have stated that if high ion beam fluxes are used in SIMS, the solid surface of the samples are subjected to damage by the ion beam. They suggested that this damage is responsible for the observed short duration of secondary ion emission from solid samples. In the liquid matrix, diffusion leads to a continuous supply of analyte molecules to the surface, so

that when the surface analyte molecules are destroyed by the incident atom or ion beam, new analyte molecules can take their place.

The use of a liquid matrix and fast atoms instead of ions resulted in the new FABMS technique. However, Burlingame (6) and Benninghoven (7), who used Cs^+ and Ar^+, respectively, as the primary ion beam in a variety of organic compounds in liquid matrices, indicate that there is no distinctive advantage of using neutral atom beams over the charged beams. Thus, the major characteristic of FABMS seems to be not the use of atoms instead of ions as the primary beam, but the use of a liquid matrix.

1.2 Neutral atom beams employed in FABMS

The three most common neutral atom beams that have been employed in FAB experiments are xenon, neon and argon. Some workers have attempted to use methane and nitrogen but with little success (8). To determine which of the above three noble gases yielded better FAB spectra, Martin and Biemann (9) studied the sample ion intensities of two peptides using these gases. They reported that the sample intensities decreased in the order of Xe, Ar and Ne. A linear plot was obtained when the intensity of protonated molecular ion (MH^+) was plotted against the molecular weight of the bombarding gas.

Similar experiments were performed by Morris and Haskins (10) using several organic analytes which included peptides, glycopeptides and antibiotics. In all these cases the most intense analyte peaks were obtained with Xe, followed by Ar and Ne. Additional work by other investigators have supported the above findings, i.e., in most instances the intensities of the MH^+ ions increased with increasing molecular weight of the bombarding particles.

K. Rinehart (11) has reported that Xe yields sample ion intensities which are about three times greater than the ion intensities produced when Ne or Ar is used as the bombarding atom beam.

1.3 The influence of the angle of incidence on intensity

It has been reported by McNeal (12) that the maximum intensity of secondary ions is obtained when there is a near-grazing collision of the ion or atom beam with the liquid surface of the sample. The maximum yields of secondary ions were observed when the angle of incidence of the primary atom beam is about 15°. The angle of incidence quoted corresponds to the angle between the surface and the primary beam. These results have been reported by Sedgewick (13) who also have found that the optimum angle

of incidence is 15°. Barber has reported on several occasions that he has used an angle of incidence of about 20° (14).

The results obtained by Martin and Biemann (9) did not agree with the above findings. Several experiments were performed under the same operating conditions, the only variable being the angle of incidence. These experiments were repeated several times with various samples. The maximum intensity was observed in all these experiments at an angle of incidence of 30°.

The causes for this disagreement are not clear. The optimum angle of incidence probably depends also on some operating parameters that were not specified by the authors, i.e., it is uncertain whether the two values mentioned above were obtained under exactly the same operating conditions. For example, the quantity of the sample applied on the probe tip or the position of the probe tip within the ion source may have been different.

1.4 Role of the matrix in FABMS analysis

It has been generally accepted that certain characteristics of the matrix play a major role in the FAB ionization process.

1.4.1 Solubility

The solubility of the analyte in the matrix is a critical factor in FABMS. It has been reported on several occasions (15, 16) that analytes which did not dissolve in the matrix led to poor FAB spectra. The addition of acids to basic samples and bases to acidic samples has helped the solubility problem to some extent. Sonication of the sample for some time has often increased the solubility of the analyte in the matrix used. In one instance a solubilizing agent (Triton X 100) had been used with chlorophyll A in glycerol to obtain a FAB spectrum (15). It is assumed that when the solubility of the analyte increases in the matrix, the homogeniety of the analyte in the sample mixture is increased. This may result in the analyte being present to the incident atom beam at a high mobile surface concentration (13).

1.4.2 Volatility

It has been possible, with low vapour pressure liquid matrices, to scan secondary ions for several minutes (15). Barber has suggested (15) that a continuous presence of sufficient matrix is necessary for this purpose. He assumes that the presence of the matrix ensures the diffusion of analyte molecules to the surface and also acts as a reservoir of unirradiated material.

1.4.3 Viscosity

FAB spectra of an oligopeptide (M = 823) in a series of polyethylene glycols (PEG) with differing molecular weights and viscosities were obtained by Przybylski (17). He observed that the intensity of MH^+ was highest when the peptide was dissolved in the PEG which had the lowest molecular weight. The intensity of the MH^+ decreased markedly when the peptide was dissolved in polyethylene glycols which had higher molecular weights. The increase in molecular weights corresponded to an increase in viscosity of the PEG's. Thus, Przybylski concluded that to obtain good FAB spectra it is necessary for the matrix to have suitable fluidity or mobility characteristics. He believes that this permits the analyte molecules to diffuse to the surface of the matrix with little hindrance.

1.4.4 Basicity (or the proton affinity)

A criterion used in the selection of a matrix is its proton affinity (P.A.) or its basicity.

The proton affinity of molecule B is defined as $\Delta H°$ of the following reaction:

$$BH^+ \longrightarrow B + H^+ \qquad (2)$$

The basicity of B is $\Delta G°$ of the above reaction.

Low intensities of analyte peaks MH^+ in comparison to matrix peaks LH^+ have been observed when proton affinity of the analyte was low. Thus, Germain Puzo and Jean Prome (18) have used α,α-trehalose as an analyte sample in glycerol, diethanolamine (DEA) and in triethanolamine (TEA) to demonstrate the influence of P.A. on the intensities of the analyte peaks. If the relative proton affinity between the trehalose and the matrix determines the intermolecular proton transfer between the analyte sample and the matrix, one would expect to observe a change in the peak intensities of the analyte as the proton affinity of the matrix is increased.

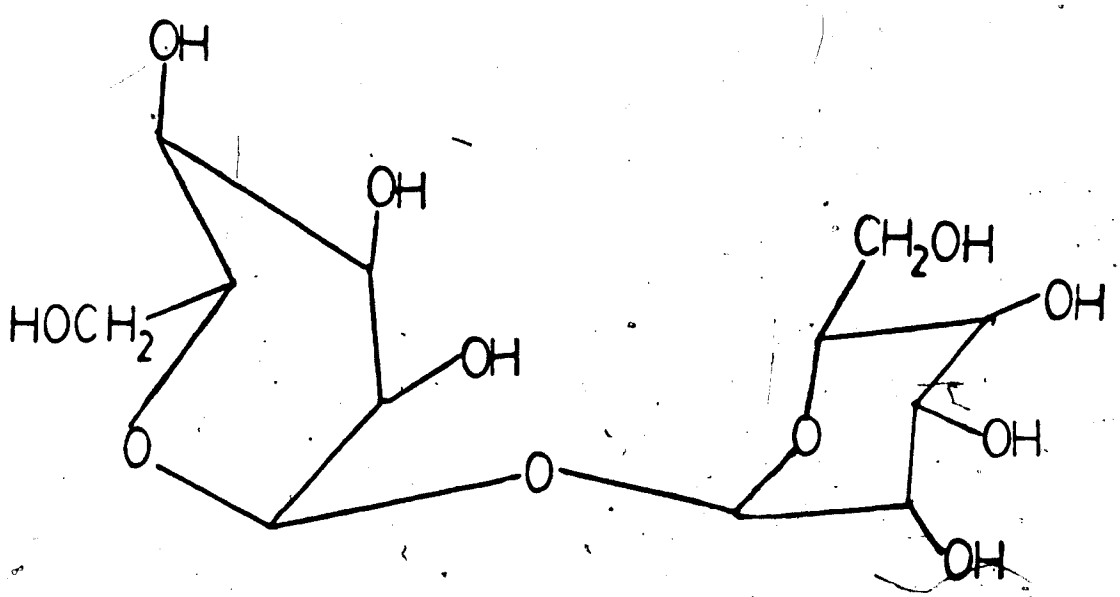

Trehalose

Trehalose, which has more basic sites than the glycerols, could be expected to have a higher proton affinity than glycerol. The FAB spectrum of trehalose (Tre) in glycerol shows no peak at 93 corresponding to $GlyH^+$ but has a fairly strong peak at 343 $(TreH)^+$. On the other hand, the spectra of trehalose in DEA and TEA are completely dominated by the matrix peaks and the analyte peaks had completely disappeared.

The influence of proton affinity on pseudomolecular ion intensities has been further illustrated by Dallinga and Nibbering (19). The following two acids have been considered by them for this purpose:

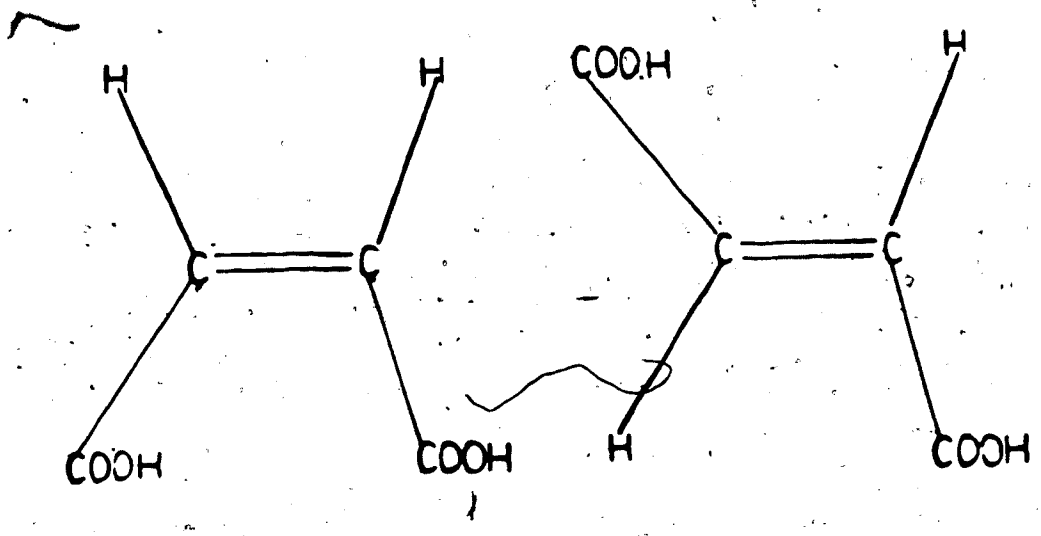

(X) Maleic Acid (Y) Fumaric Acid

They observed that the peak intensities due to (Y) were about 50 - 100 times less than the corresponding peaks of (X) in glycerol. The difference in peak intensities of the two acids has been rationalized by the authors as follows: the (X) acid having two-COOH groups in the cis position has the ability to form a proton-bridged complex (Z) as shown below.

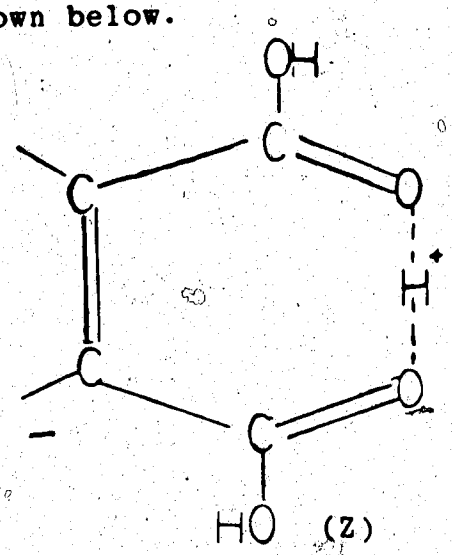

(Z)

1.5 Commonly used matrices for FAB

The important characteristics of a FAB matrix have already been discussed. Some of the more widely used matrices are listed below.

1.5.1 Glycerol (Gly) [$HOCH_2CH(OH)CH_2OH$]

This was the original matrix compound used in FAB experiments, and is still the most versatile matrix. The

major peaks of glycerol are MH^+ (m/e = 93) and cluster peaks [MH^+ + $(M)_x$] when x = 1, 2 or 3. A wide variety of compounds such as peptides, nucleotides, carbohydrates and porphyrins yield good FAB spectra when dissolved in glycerol (16). Its high boiling point and its ability to dissolve moderately polar to very polar compounds render this as an excellent matrix for many samples.

1.5.2 Thioglycerol [$HOCH_2CH(OH)CH_2SH$]

Certain antibiotics and polysaccharides give good FAB spectra in thioglycerol (16, 20). Lehman and Kong have reported (21) that angiotensin, an oligopeptide, dissolved in thioglycerol produced ion intensities which were about ten times greater than those obtained when the peptide was dissolved in glycerol. The authors also observed that the FAB spectra of other oligopeptides in thioglycerol were generally better than the FAB spectra in glycerol. A minor disadvantage of this matrix compound is its odour.

1.5.3 3-Nitrobenzyl alcohol (NOBA)

($3\text{-}O_2NC_6H_4CH_2OH$)

Meli and Seibl (22) have reported that NOBA has proved to be a useful matrix for analyte samples which have failed

in glycerol and thioglycerol. Thus, a cyclic peptide cyclosporin A, which failed to give a good FAB spectrum in glycerol, produced an excellent spectrum in NOBA, with MH^+ being the predominant peak.

1.5.4 Diethanolamine $(HOCH_2CH_2)_2NH$ and Triethanolamine $(HOCH_2CH_2)_3N$ (DEA, TEA)

DEA and TEA have been used as matrices with considerable success for some oligosaccharides (23). The principal peaks observed were the adduct ions $(M + DEA)H^+$ and $(M + TEA)H^+$.

DEA and TEA being amines could be expected to have higher P.A. values than the oligosaccharides. This may be a reason for the lack of MH^+ peaks of these analytes in DEA and TEA.

1.6 Sensitivity enhancement by matrix modification

A method that has been employed extensively by many to improve the intensity of the analyte peaks MH^+ is the addition of acids or bases to the sample solution prior to the FAB experiment (9, 17). Some of the acids that have been added are hydrochloric, oxalic, and acetic acid. Martin and Biemann (9) selected a peptide (mol. wt. 921) to illustrate this fact. The initial FAB spectra of the

peptide in glycerol showed ions only of the matrix glycerol. As the concentration of the acetic acid was increased in the sample, a corresponding increase in the intensity of the MH^+ peak was observed.

A compound known as methotrexate (MTX), which is a folic acid analog, was used by Michael Przybylski (17) to illustrate the sensitivity enhancement by the addition of acetic acid.

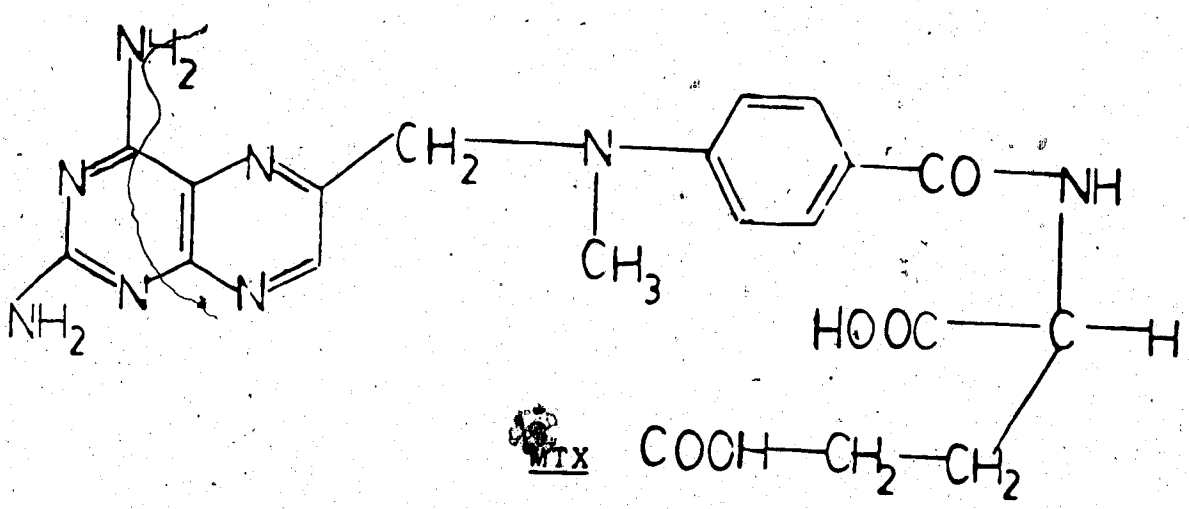

MTX

MTX in glycerol produced no MH^+ under FAB conditions. The addition of acetic acid to this mixture resulted in an increase in intensity of the MH^+ peak.

When a base (M) is added to an acid (HX), the ions MH^+ and X^- are formed in solution. It was assumed that such reactions did take place in the above experiments, "preforming" the ions MH^+ in solution prior to the FAB

experiment. The enhancement of the intensity of MH^+ ions was assumed to be due to the FAB induced desorption of MH^+ ions present in the liquid matrix. The presence of MH^+ in the matrix has been termed "preionization" by the FAB practitioners (15, 24). The fact that in most cases there is an enhancement of the intensity of MH^+ or $(M - H)^-$ when preformed ions are present in the matrix has led to the "precursor model" described next.

CHAPTER II

2.0 Ionization models for FABMS

2.1.1 Precursor model - SIMS of solids

When a fast atom or ion collides with a solid or a liquid surface, the kinetic energy and momentum of the projectile is transferred to an area near the point of impact. This energy will be dissipated by a collision cascade process within the sample. According to Benninghoven (7) such a transfer of energy creates an "excited area" near the point of impact (Figure 1). The emission of secondary ions is thought to occur by the transfer of kinetic energy to a preformed ion (precursor) near the surface of the excited area.

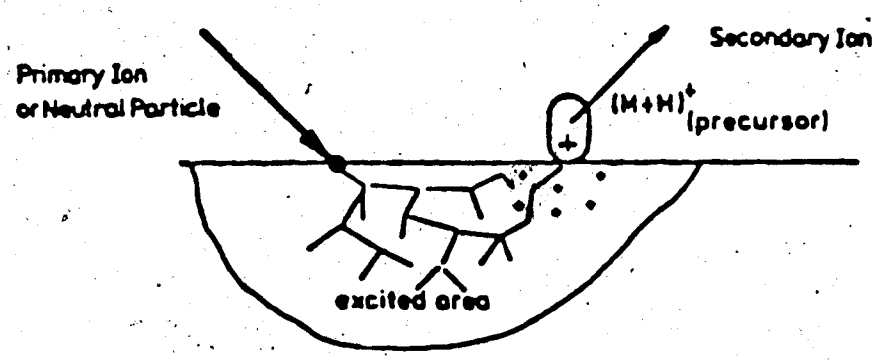

Figure 1: Ejection of Secondary Ion in the Precursor Model

The emission of secondary ions may be dependent upon the size of this excited area and the efficiency of energy transfer from the bombarding particles to the preformed ions (7). Magee has put forward (25) two possible ways that a particle from the surface of the sample can be ejected upon bombardment by fast atoms or ions. They are the: (i) direct knock-on; (ii) linear cascade methods.

(i) Direct Knock-on: In this instance, the bombarding particle transfers energy to a sample atom which, after undergoing a small number of collisions near the surface of the sample, is ejected from the surface.

(ii) Linear Cascade: Here, the sample atoms, after the initial impact of the primary atom beam, will undergo a cascade of collisions which will penetrate deeper into the sample. Some of these atoms may recoil towards the surface with adequate energy to be ejected from the surface of the sample.

2.1.2 Precursor model - preformed ions in liquid matrices

It was pointed out in the preceeding section (1.6) that the presence of preformed ions MH^+ in the liquid

matrix leads to an increase of the intensity of the MH^+ and other related ions in the FAB spectrum. On the basis of such observations, Benninghoven (7) has extended the precursor model for solids to liquid matrices. Benninghoven assumes that the emission of preformed ions is a result of a fast transfer of kinetic energy in the collision cascade to a preformed ion.

Contrary to the above model, which assumes that pre-ionization is essential in the ionization process of FABMS (24), it has been reported by Barber and Tyler (15) that nonionic compounds like saturated aliphatic hydrocarbons such as $C_{16}H_{34}$, $C_{18}H_{38}$ and $C_{20}H_{42}$ have produced good FAB spectra.

The Desorption Ionization (D.I.) Model (4, 26) described next is a further extension of the above model which attempts to explain two additional processes that occur in FABMS.

2.2 Desorption ionization model (D.I. model)

This model proposed by Cooks (4, 26) explains the secondary ion formation in SIMS and FAB as a desorption of ions and molecules directly from a solid or a liquid phase, into the vacuum. In this model Cooks has defined two zones of activity. They are the "Selvedge" and the vacuum

regions. Selvedge has been described as the near surface region of the sample. He assumes that there are three processes that occur upon bombardment to give rise to secondary ions:

(i) Direct desorption of preformed ions C^+ or A^- from the surface to the vacuum region. It is believed that this occurs by energy and momentum transfer from this primary atom or ion beam to the surface ions.

(ii) Neutral molecules (M) which are also desorbed as a result of the bombardment may interact with free electrons which are generated by the impact of fast atoms, to produce $\dot{M}^+$ or $\dot{M}^-$ - Electron Ionization.

(iii) Cationization or anionization reactions, where the neutral molecule M may form cluster ions $(M + C)^+$ or $(M + A)^-$ - Ion Molecule reactions.

It is assumed that ion molecule reactions (iii) and electron ionization reactions (ii) occur in the "Selvedge" region. It is also suggested that these secondary ions could dissociate in the vacuum region to produce fragment ions. According to this model the desorption and ionization are considered to be two separate processes. The analyte if charged, may be desorbed as an ion. If

desorbed as a neutral, it may be ionized by the reaction with a desorbed ion or an electron (4).

2.3 Gas phase collision model (G.C.M.)

Michl (27) had observed that when low temperature solids of Ar, Kr, Xe and CO_2 were bombarded by ions such as He^+, Xe^+ and Ar^+, considerable amounts of both positive and negative ion clusters were observed. It was also noted that sometimes the stoichiometry of such clusters had no relevance to the molecular composition of the bombarded solid. To explain such observations, Jonkman and Michl (28) have proposed the following model. Although the Jonkman, Michl model is primarily meant to explain the ionization process in molecular solids upon bombardment, they are of the opinion that this model is also applicable to FABMS.

When keV energy primary ions or atoms bombard a surface, they will cause the ionization of some molecules at the top surface layers of the solid. This is due to the energy and momentum transfer from the primary ions or atoms to the surface molecules of the solid. The secondary ions thus formed have been defined by Jonkman and Michl (27, 29) as the "first batch" of secondary ions. It is assumed that the probability of these secondary ions reacting with the

other molecules of the solid is low. The primary ions or atoms that penetrate into the solid will undergo a cascade of collisions. Following the collision cascade, many molecules will acquire an excess of kinetic energy which is slaked by the energy transfer to the surrounding molecules.

Due to the above processes, a thermally activated tract ("thermal spike") is formed near the region of impact (27). This region behaves as a high pressure, high density and a high temperature gas. The collision cascade and the subsequent formation of the "thermal spike" allow sufficient time for the hot molecules and ions produced by the collision cascade to chemically react with one another. Such reactions ultimately may lead to the formation of positively or negatively charged cluster ions. The number of chemical reactions that are caused by a single impact event is not known. When Michl (29) bombarded solid NO with 4 keV Ar^+, the major cluster ion observed was $[NO(N_2O_3)_n]^+$. Based on the composition of such clusters, they have concluded that the number of chemical reactions molecules undergo could be a few dozen.

The ejection of these secondary ions has been described by Michl (27) as an explosive expansion of a high pressure gas into the vacuum. This process will cause a rapid cooling of the hot gas.

It has been suggested by Michl and Jonkman (28) that molecular ions and cluster ions may undergo further fragmentations or rearrangements on their way through the spectrometer.

Our experiments, which will be discussed in later chapters, were performed with a view to obtaining a better understanding of the mechanism of ionization in FABMS and to determine which of the above models, if any, is more appropriate. A better understanding of the process leading to the formation of FAB mass spectra should ultimately lead to rational rather than purely empirical methods of finding the optimal conditions for analytical purposes using FABMS.

CHAPTER III

EXPERIMENTAL

3.1 General description

An AEI/Kratos MS9 double focussing mass spectrometer equipped with a FAB gun was used in all the experiments. The double focussing mass spectrometer consists of the following main elements: (i) Ion source; (ii) Analyzer; (iii) Vacuum system; (iv) Detector. A schematic diagram of a double focussing mass spectrometer ion source, analyzer system and detector is shown in Figure 2.

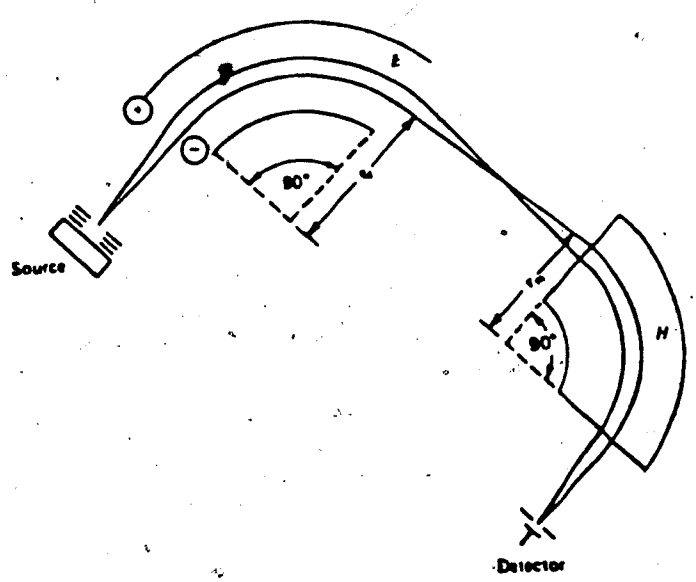

Figure 2. Nier-Johnson double-focussing mass analyzer. E = electric field. H = magnetic field.

3.2 Fast atom bombardment gun (FAB gun)

A FAB gun is employed to generate a beam of fast atoms of a particular gas. The FAB gun used in this laboratory was developed by A. Hogg (30). It is a cold cathode source which is also known as a saddle field source (see Figure 3). It consists of two cylindrical aluminum cathodes

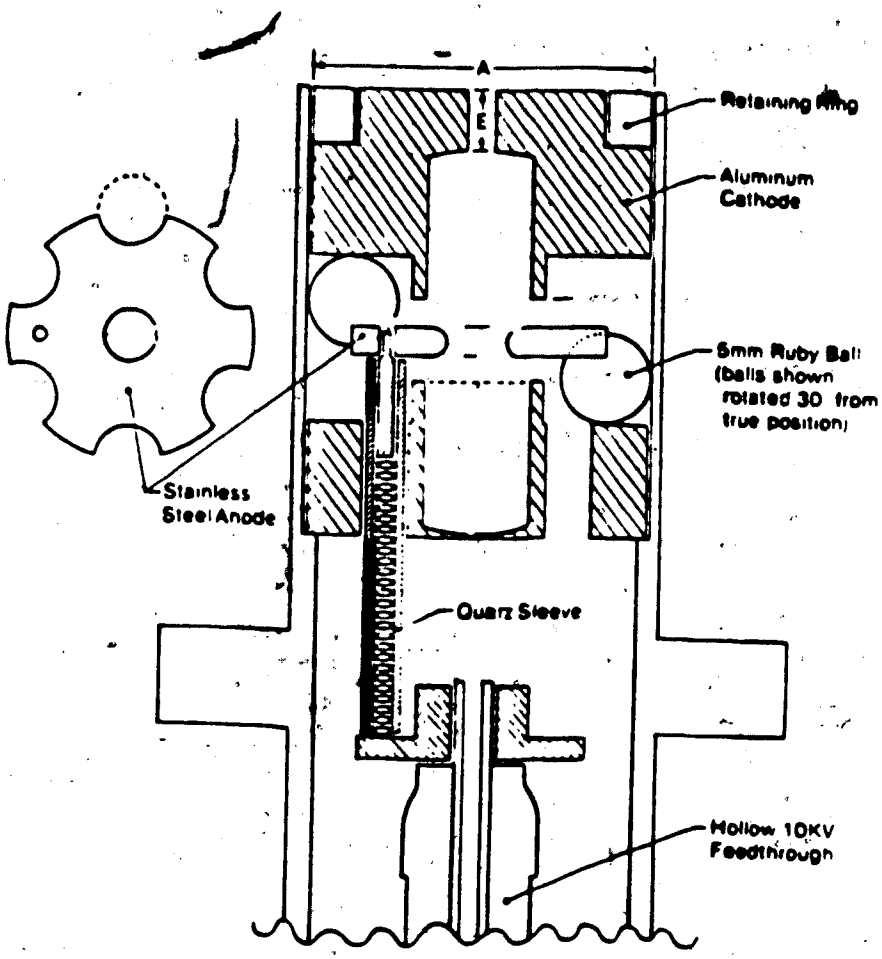

Figure 3. Schematic diagram of FAB gun showing internal structure.

(negative poles) and a circular stainless-steel anode (positive pole). The anode with six semi-circular notches has a hole in the center. This hole creates a saddle in the potential field through which the electrons producing the ionization will oscillate. The first few electrons initiating the discharge originate from background ionizing radiation. One of the cathodes has a single central channel to permit the exit of atoms or ions. The other has two channels, one to permit the electrical connection to the anode and the other for the gas to enter. Insulation between the two cathodes and the anode is provided by six ruby balls. A schematic diagram of the FAB gun is shown in Figure 3 [30]. Xenon is supplied to the FAB gun via a rubber tube at a pressure of about 0.5 lb in.$^{-2}$. The flow of gas into the gun is controlled by a needle valve.

The anode is normally held at a potential of about +8kV and the cathodes at 0 volts. The oscillating electrons ionize the Xe atoms producing the Xe ions. The ions that originate at or near the anode are accelerated by the potential field between the cathodes and the anode. Only the ions that are accelerated between the upper cathode and the anode reach the exit (E). A charge exchange occurs between the fast ions and the atoms with little change in forward momentum as follows:

$$Xe^{+}_{\alpha} + Xe^{\bullet}_{\beta} \longrightarrow Xe^{\bullet}_{\alpha} + Xe^{+}_{\beta}$$

Fast Fast

The above charge exchange should occur near or the exit hole to obtain the maximum flux of the fast atoms.

3.3 Ion source

The ion source consists of a probe tip made of Cu and a pair of ion extraction plates, both of which are held at the full accelerating voltage of 8 kV. A schematic diagram of the ion source is shown below (Figure 4).

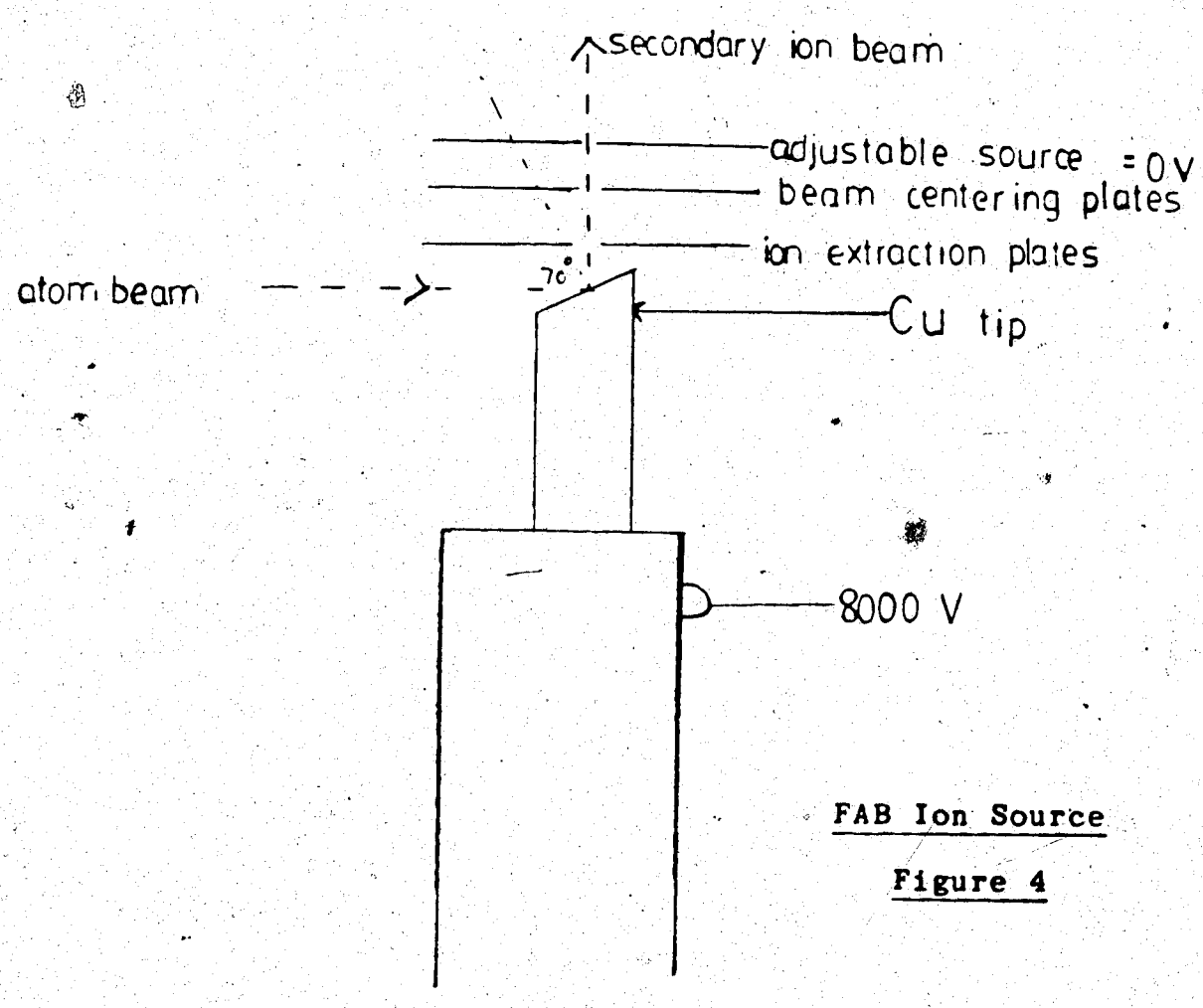

FAB Ion Source

Figure 4

The probe tip is also held at the full accelerating voltage by means of a copper spring contact which is attached to the ion extraction plates. The probe is inserted through an axial lock in a direction coaxial with the secondary ion beam. However, the tip of the probe is machined at an angle of 20° (see Figure above). The atom beam has an angle of incidence of 70° relative to the normal of the probe surface. The beam centering plates are held at a potential of about 7500 volts. The potential field thus created between the beam centering plates and the ion extraction plates is assumed to extract secondary ions produced near the surface of the copper tip. Further acceleration of the secondary ions is provided by the voltage drop between the beam centering plates and the adjustable source plates which are at earth potential.

3.4 The analyzer

The analyzer consists of the electrostatic analyzer (E.S.A.) and the magnetic analyzer.

3.4.1 E.S.A.

The E.S.A. consists of a pair of smooth, curved metals across which a potential is maintained. The ions originating in the source have a small spread of kinetic

energy before entering the E.S.A. due to the ionization process and other factors. An ion entering the E.S.A. will be deflected by the electric field created between the two plates. The result is a circular orbit of the ion with a radius r_e which is equal to $mv^2/e.E$; m = mass of ion, v = velocity ~~of ion~~, e = charge, E = electric field. Thus, the deflection produced by the electric field is proportional to the kinetic energy of the ion. Ions of different energies therefore emerge from the E.S.A. on different paths, and enter the magnetic analyzer.

3.4.2 Magnetic analyzer

When these ions enter the magnetic sector with a magnetic field (B), the ions experience a force evB which is normal to the direction of motion. The result is a circular orbit of the ion, with a radius r. Then:

$$evB = mv^2/r \qquad (3)$$

Therefore: $$r = mv/eB \qquad (4)$$

Thus, the radius taken by an ion in the magnetic sector is dependent on its mass to charge ratio. By continuously varying the magnetic field (B), each m/e species is successively focussed at the same point.

3.5 Detection of ions

The device that is used for the detection of ions is known as the electron multiplier. It consists of dynodes made of a material (e.g., Cu/Be alloy) which has the property of emitting secondary electrons when bombarded with energetic particles. An amplification of more than 10^6 can be achieved by a cascade effect of electrons producing more electrons from the initial impact of the secondary ions. The signal from the multiplier is fed to an analog to digital converter before being stored in a computer.

The interfacing of the mass spectrometer with the computer by an analog to digital converter, the Data General Nova 4/x computer, and the data acquisition and processing software are known as the Kratos DS-55 system. The DS-55 consists of an integrated and an interrelated set of programs which run under the control of the Data General's Real Time Disk Operating System (RDOS). RDOS is a general operating system. It also provides commands which can be used for deleting scans or runs, backing data up to magnetic tapes or cassettes and restoring it to disks. Some of the command words used in a typical run are:

(i) Plot: This plots the mass vs. intensity for a range of peaks in each scan specified by the user.

(ii) LCALB: A calibration program for low resolution experiments.

(iii) QUAN: A quantitative report which prints a wide range of information about all the peaks in each scan specified by the user.

(iv) PKAVG: Averages scans together to obtain more accurate mass or intensity information.

3.6 Experimental conditions, procedures and reagents

The FAB gun was operated with xenon as the bombarding gas. The flow of gas was adjusted to obtain a discharge current of 1 mA and a voltage of 8 kV except when the Total Ion Current (TIC) measurements were made. A discharge current of 0.6 mA and a voltage of 7 kV was used in this instance. A low voltage was used in order to minimize rapid fluctuations in total ion currents.

The total ion currents were measured by means of a Keithley 610C electrometer. The power supply to the E.S.A. plates was removed before the electrometer was connected to the two plates. In the absence of an electric field between these two plates, all the ions produced in the ion source will collide with the upper plate of the E.S.A. The

electrometer was used in the charge mode and the output was recorded on a strip chart recorder. The current was obtained from the initial slope of the curve. The time allowed for the charge buildup was about 2 minutes. The average of 3 TIC measurements was obtained for each sample using pure glycerol as the reference, alternately. The relative standard deviation of the TIC measurements was typically in the range of 5 to 10 percent.

Certain samples did not dissolve in some matrices even after the samples were vigorously stirred. These sample mixtures had to be warmed in order to dissolve the analytes. The volumes of the sample mixtures ranged from about 0.5 ml to about 5 mls. The liquid mixtures were applied on the copper tip with a spatula to obtain a thin uniform layer. The amount applied on the tip varied between 3-5 μl. The area of the copper tip was calculated to be approximately 0.1 cm^2. Assuming the layer on the to be uniform, the thickness of this sample layer is found to be about 0.2 mm.

The chemicals used in these experiements were all laboratory reagent grade, and were used as received.

CHAPTER IV

RESULTS AND DISCUSSION

4.1 Verification of the role of proton affinity in FABMS

As already explained in the introduction, a criterion normally considered in the selection of a matrix is its proton affinity (P.A.), but so far, no systematic experiments have been performed to determine the influence of the proton affinity of analytes and matrices on the relative intensities in FABMS spectra. Therefore, we have carried out the following FABMS experiments. Six compounds which have a wide range of proton affinities were chosen for the FAB experiments:

(i) 3 - Nitrobenzyl alcohol (NOBA)

(ii) Glycerol

(iii) 1,2,4 - Butanetriol [$HOCH_2CH_2CH(OH)CH_2OH$]

(iv) P - Octylaniline [$CH_3(CH_2)_7C_6H_4NH_2$]

(v) Diethanolamine (DEA)

(vi) Triethanolamine (TEA)

Binary solutions consisting of 10 mole percent of one of these compounds, called the analyte M in 90 mole percent of the other compound, called the matrix L, were used in the FAB experiments. The results of the experiments are

presented in Table 1. The proton affinities, gas phase basicities, and entropy changes on protonation of the compounds were obtained by J. Sunner from this laboratory in separate experiments with a pulsed high pressure ion source mass spectrometer (31). The analyte and matrix compounds in Table 1 are arranged horizontally and vertically in the order of increasing proton affinities in the gas phase. The values in the table correspond to the intensities of the analyte and matrix derived ions as a percent of the total ionization. The upper number of each pair relates to the analyte and the lower number to the matrix.

The major peaks observed of these compounds are the MH^+, M_2H^+, $(ML)H^+$, $MH^+ - H_2O$ (in the alcohols) and fragment peaks of MH^+. The FABMS spectra of some of the mixtures are shown in Figures 5 - 7 (TEA in NOBA Figure 5, glycerol in TEA Figure 6, and glycerol in octylaniline Figure 7). The major peaks of the matrices L are the LH^+ and the L_2H^+. The predominant analyte peak in Figure 5 (TEA in NOBA) is $(TEA)H^+$ (m/e = 150). The intensities of the analyte peaks $GlyH^+$ (m/e = 93) in Figures 2 and 3 (Gly in TEA and Gly in octylaniline) are negligible.

Table 1: Summary of FAB spectra[a] of 10% (mole) binary mixtures

Matrix	PA/(Kcal mol^{-1})[d]	Basicity at 300K[e] /(kcal mol^{-1})	Analyte: NOBA	Glycerol	Butanetriol	4-Octylaniline	Diethanolamine	Triethanolamine
3-Nitrobenzyl alcohol (NOBA)	194	186	20	5 20	17 9	33 1	44 4	45 0
Glycerol	209	196	7 14	35	26 7	41 0	7 2	19 1
1, 2, 4 - Butanetriol	216	201	1 32	0 36	31	34 3	27 12	45 0
4 - Octylaniline	214	206	1 41	1 44	1 45	39	5[c] 43[c]	12 35
Diethanolamine (DEA)	228	220	0 46	0 57	0 68	25[c] 18[c]	52	15 28
Triethanolamine (TEA)	223[b]	225[b]	0 57	0 60	0 39	11 30	2 35	48

a) The numbers in the table give the contribution from matrix and analyte, respectively, to the FAB spectrum, expressed as percentages of total ionization. The lower number refers to the matrix and the upper number to the analyte. Only the major ions were included. Their masses are as follows: NOBA: 154, 136, 307; glycerol: 93, 185; 1,2,4 - butanetriol: 107, 89, 79, 213; 4 - octylaniline: 206, 205, 106; DEA: 106, 211; TEA: 150, 148, 118. The intensities of mixed clusters were generally small. The concentration of the analyte was 10 $\pm$ 1 mole %.

b) Estimated. Proton transfer equilibria could not be measured since the vapour pressure was too low.

c) The intensity of peak at m/e = 106 was divided up between DEA and octylaniline.

d) The proton affinity of M corresponds to the ΔH° for the process $MH^{+} = M + H^{+}$, at 300 K.

e) The gas phase basicity of M corresponds to ΔG° for the process $MH^{+} = M + H^{+}$, at 300 K.

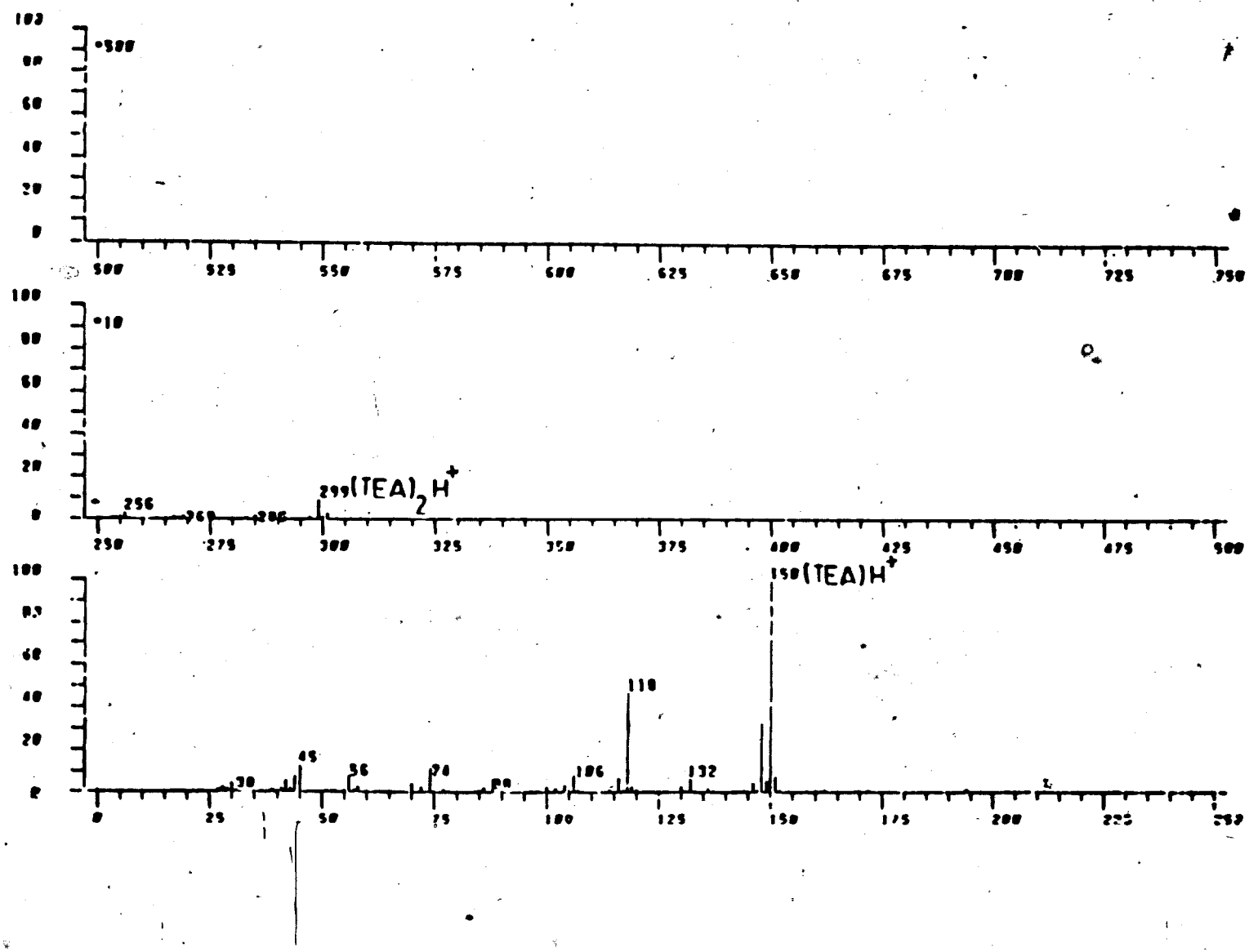

Figure 5 FAB spectrum of 10 mole percent TEA in NOBA.

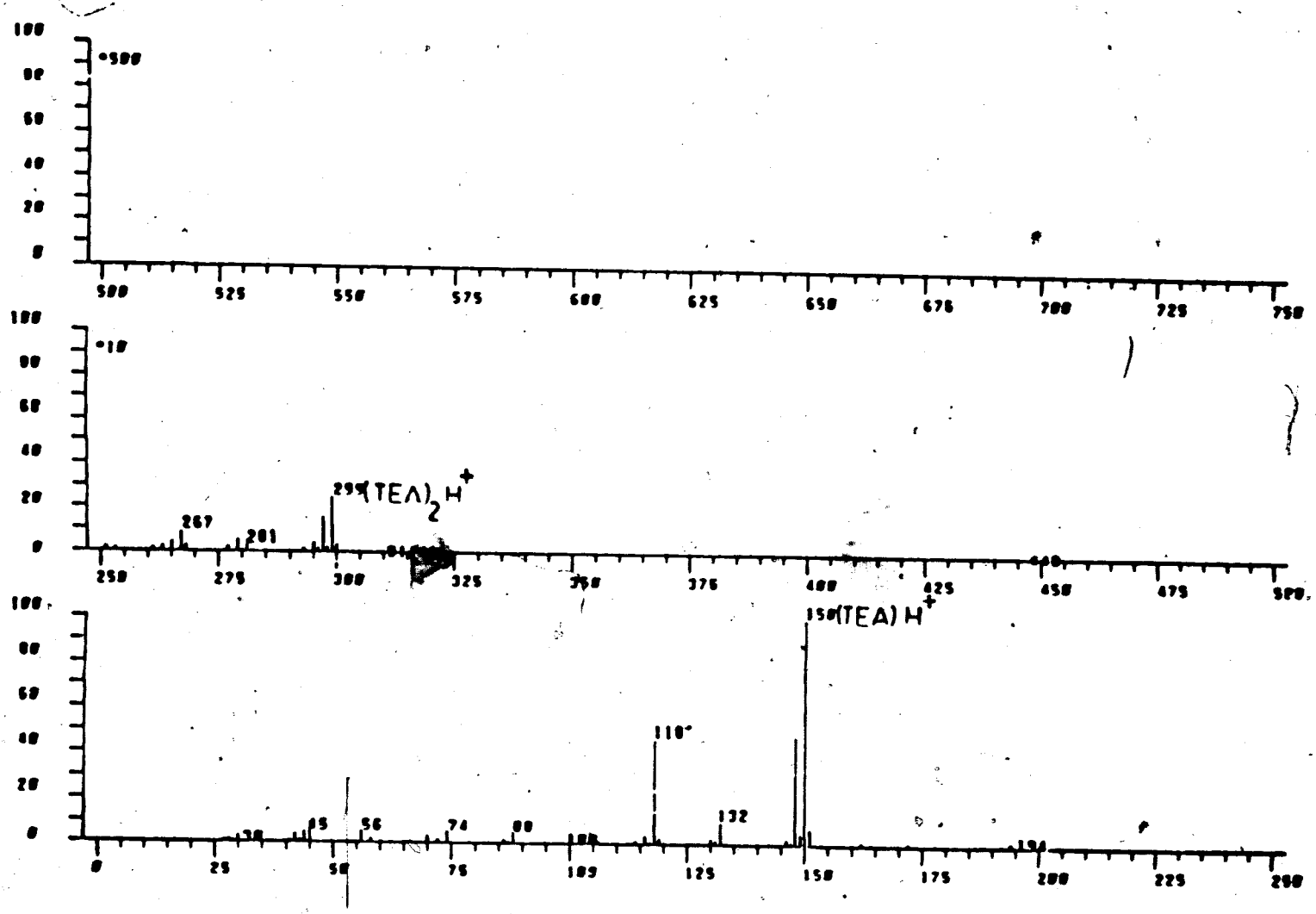

Figure 6 FAB spectrum of 10 mole percent glycerol in TEA.

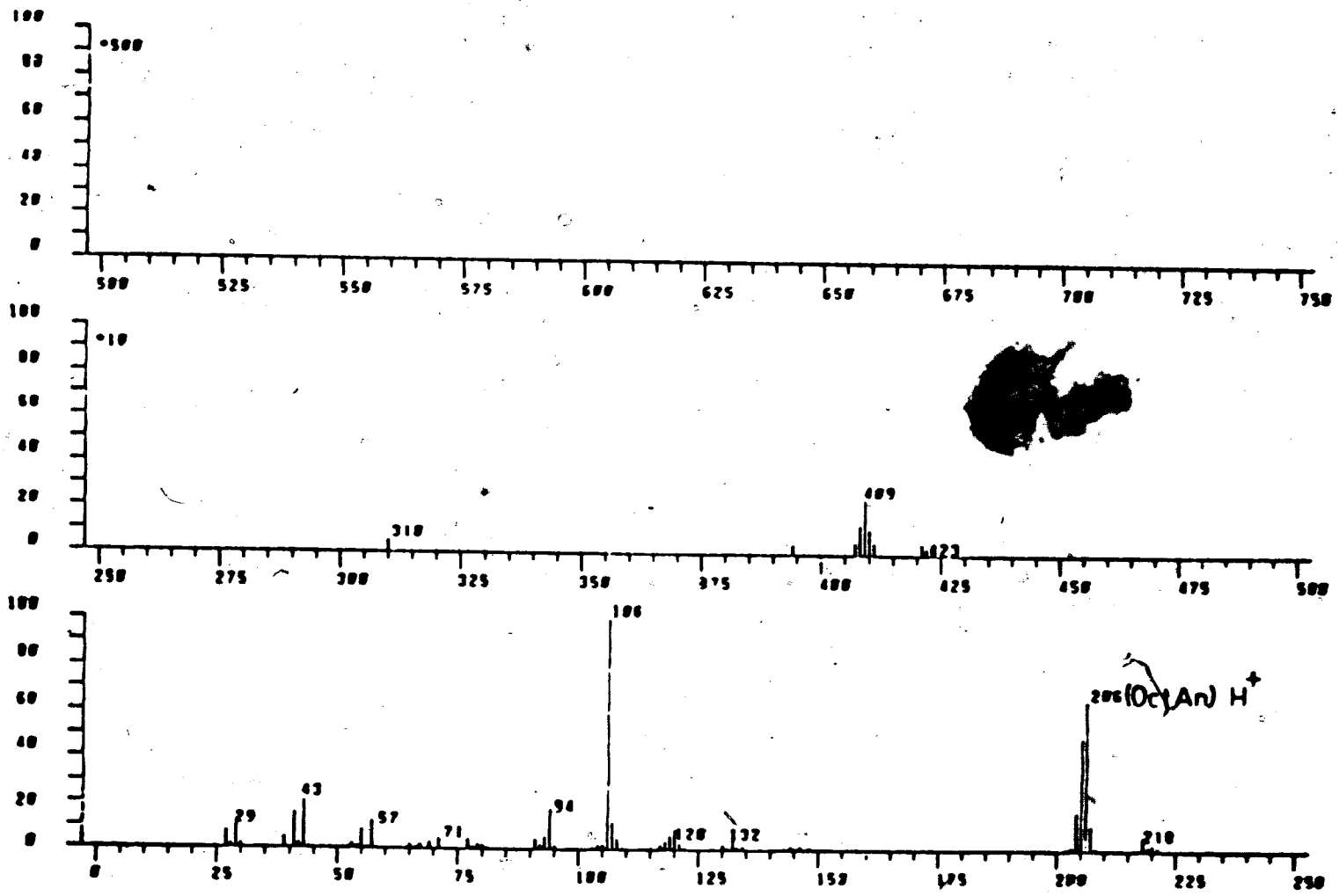

Figure 7 FAB spectrum of 10 mole percent glycerol in octylaniline.

Inspection of Table 1 shows that the ions derived from the more basic compound are generally dominant. It is also quite apparent that there is a definite correlation between the intensities of the analyte ions and the P.A. differences between the analytes and the matrices. When moving across Table 1, one is comparing spectra of analytes with progressively increasing basicities in a fixed matrix. It is clearly seen that the intensities due to the analyte ions increase while those for the matrix ions decrease. Consequently, the ratio of analyte ions to the matrix ions also increases quite considerably across the table. Similarly, when moving down a column one is comparing the intensities for a fixed analyte in different matrices of increasing basicities. The intensity of the analyte ions decreases relative to the matrix ions, i.e., the ratio of the analyte ions to the matrix ions decreases down a column. This means that the ratio of the analyte to the matrix ion intensities is highest at the upper right corner of the table where the analyte which has the highest basicity value is dissolved in a matrix with the lowest basicity value. The lowest ratio is at the bottom left corner where the analytes with the lowest basicity value is dissolved in a matrix with the highest basicity value.

The only exceptions to these results are the sample mixtures containing 10 mole percent 4 - octylaniline in glycerol and in butanetriol. The aniline was not soluble in these two matrices. The low solubility of the aniline in the alcohol matrices may be due to the hydrophobic octyl group of the aniline. Since the density of the aniline is lower than that of the two alcohols, one could expect the aniline to form the top layer on the probe tip when the sample mixtures are applied on the surface of the probe tip. This would mean that the molecules that are exposed to the bombarding atoms would predominantly be the aniline molecules. This would explain the high intensity of the aniline derived ions in these spectra. Generally, the intensity of the dimer, M_2H^+, over the intensity of the pseudomolecular ion, MH^+, is much lower when M is an analyte molecule than when M is a matrix molecule. However, in the case of octylaniline, the monomer to dimer ratios are similar, irrespective of whether the aniline is used as an analyte or a matrix. Since the sample surface is enriched with the aniline, the aniline molecules that are desorbed from the sample surface due to the fast atom bombardment have a greater probability of interacting with other desorbed aniline molecules to form the proton bound dimers. In other cases, where the analyte is well

dissolved in a matrix, the desorbed analyte molecules may have a lesser probability of interacting with the other desorbed analyte molecules due to the large number of matrix molecules that are also present.

4.2 Preference factors

The degree of preference for the analyte over the matrix in a binary mixture in FABMS can be expressed as a "preference factor" (P.F.).

$$\text{P.F.} = \frac{\text{Total intensity of analyte ion peaks}}{\text{Total intensity of matrix ion peaks}} \times \frac{\text{moles of matrix}}{\text{moles of analyte}}$$

The preference factors are highest in the upper right corner and lowest in the bottom left corner in Table 1. The preference factors remained relatively constant even when the concentration of the analyte was decreased by a factor of 100. For example, when the mole percent of TEA in glycerol was decreased from 10% to 0.1%, there was no significant difference in the preference factors between these two samples.

Even though the preference factors for a given analyte in different matrices were different, the observed fragmentation pattern was relatively constant. This was true for all FAB spectra on which Table 1 is based. The pattern

was also the same when the compound was used as a matrix, with or without an analyte. This observation is illustrated in Figure 8 which depicts the FABMS spectra of TEA in two different chemical environments. Figure 8a shows the FAB spectra of pure TEA matrix and Figure 8B shows a 10 mole percent solution of TEA in NOBA. In both spectra, the predominant peak is the $(TEA)H^+$ (m/e = 150). The major fragment peaks are m/e = 148, m/e = 132 and m/e = 118. The intensities of the fragment peaks relative to the base peak (m/e = 150) are similar in both spectra. If the ionization process in FABMS occurs according to the precursor model, the intensities of the analyte and matrix derived ions are expected to depend to a great extent on their respective basicity values in the liquid phase. This is because the distribution of protons between the matrix and the analyte molecules in solution will be determined by the relative basicities of the two components. The pKa values for DEA and TEA in aqueous solutions (32) are as follows: DEA = 8.8 ($Kb = 6.3 \times 10^{-6}$) and TEA = 7.7 ($Kb = 5.0 \times 10^{-7}$). The respective proton affinities in the gas phase are 228 kcal mol^{-1} and 233 kcal mol^{-1}. Therefore, one can clearly see that the basicities of these compounds in solution is the reverse of that in the gas phase. If the protonated ions are formed in the liquid phase before being desorbed as

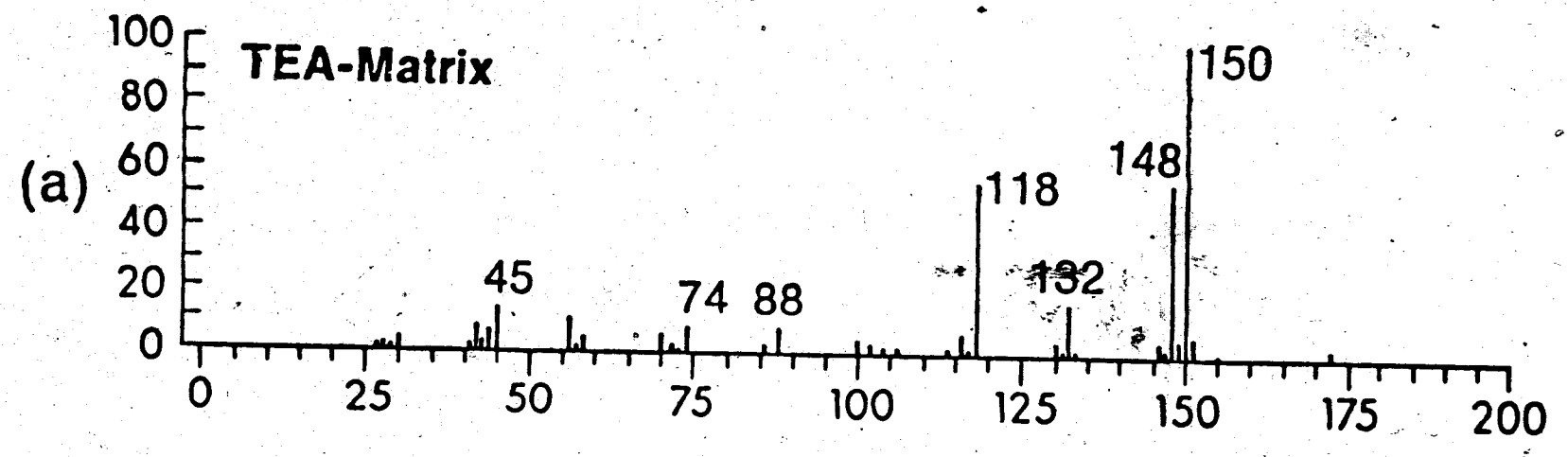

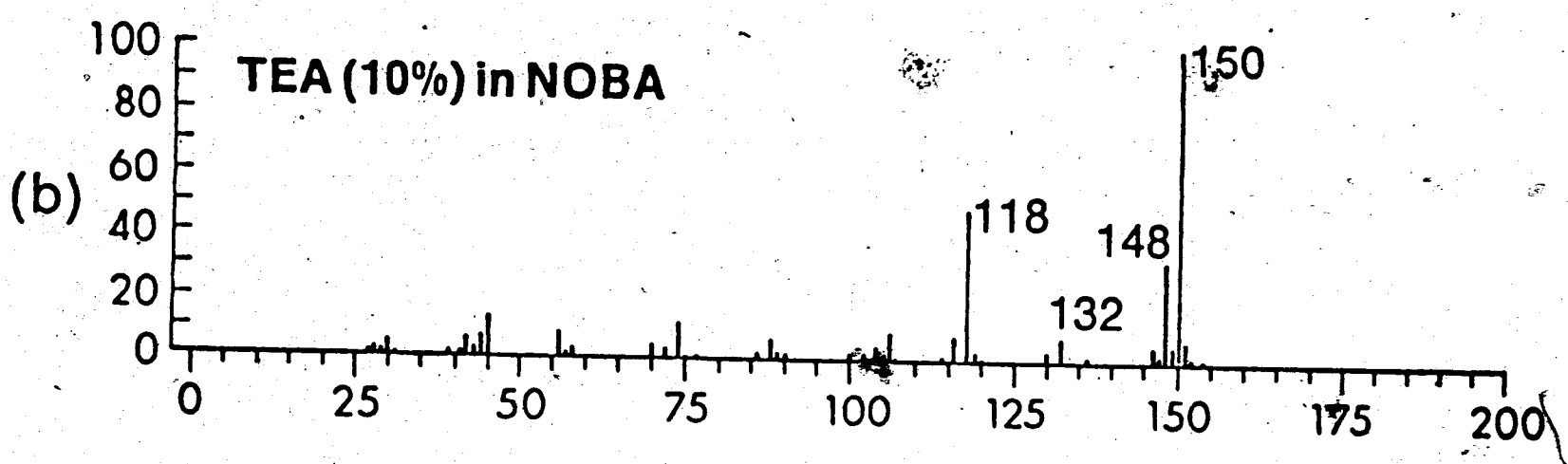

FIGURE

(8a) FAB sepctrum of neat TEA.

(8b) FAB spectrum of TEA in NOBA.

implied in the precursor model, one would expect a high degree of preference for DEA over TEA, in a 10 mole percent solution of TEA in DEA. But the results in Table 1 indicate the P.F. of TEA in DEA to be 4.8 and the P.F. of DEA in TEA to be 0.5. Since the gas phase basicity of TEA is greater than that of DEA, the only explanation for these results that could be given at this stage is that the protonation reactions may occur in the gas phase.

4.3 The relevance of the precursor model and the G.C.M. in FABMS

Even though the compounds chosen for these experiments are considered to be neutral and have negligible concentrations of preformed ions, a sufficient amount of ions could build up instantaneously on the surface of the sample when the atom beam impinges on the sample. These ions could then act as preformed ions. Magee (25) has reported that the atom flux normally employed in FAB or SIMS experiments is about 10^{13} atoms/sec. He has also assumed that the damage cross section of an atom is about 100 $A^{\bullet 2}$. The area of the probe tip we used was calculated to be about 0.1 cm^2. Therefore, the average time that would elapse between two atoms hitting the same area is about 1 second. Magee has reported (25) that when a neutral atom

beam impinges on a sample surface, the depth of the collision cascade is between 80 - 100 Å. If we assume the diffusion coefficient of a molecule in a liquid to be about 10^{-5} cm^2 sec^{-1}, the average distance the molecule will travel in one second is about 10^4 Å. This will ensure adequate time for the ions produced at the surface, due to the atom bombardment, to diffuse to a depth of more than 100 A in the bulk liquid before the same surface area is bombarded again. Therefore, the probability for a buildup of ions on the surface and the subsequent desorption of these ions is small. Thus, our experimental results do not favour a precursor model but instead tend to agree with a gas phase collision model.

Since the concentration of the matrix is much greater than the analyte in the sample solutions we used, there will be more of the protonated matrix molecules due to the collisions of the matrix molecules with ionic fragments. Since analyte molecules which have a higher proton affinity than the matrix produced high preference factors ($\approx$ 100), it must mean that the initially protonated matrix molecules undergo a number of gas phase collisions ($\approx$ 10) with the surrounding intact molecules.

Figure 9c shows the FAB spectra of the pure glycerol. Figures 9b and 9a show the chemical ionization (CI) mass

spectra of glycerol, where glycerol has been protonated by CH_5^+ and $C_6H_7^+$, respectively. These CI spectra were obtained in separate experiments performed in this laboratory by J. Sunner using a high pressure ion source mass spectrometer. The exothermicities of reaction (5) and (6) involved in the protonation under methane CI conditions are given below (31).

$$\text{Glycerol} + CH_5^+ \longrightarrow (Gly)H^+ + CH_4 \qquad (5)\ \Delta H = -77\ \text{kcal/mole}$$

$$\text{Glycerol} + C_6H_7^+ \longrightarrow (Gly)H^+ + C_6H_6 \qquad (6)\ \Delta H = -28\ \text{kcal/mole}$$

The reaction with the higher exothermicity will lead to products with greater internal excitation energy. As a result, the products of this reaction should be fragmented to a larger degree. The fragment peak m/e = 75^+ in Figure 9b is much more intense than that of Figure 9c. In addition to the peak at 75^+, fragment peaks appear at m/e = 57^+ and 45^+ in Figure 9b, which are not observed in Figure 9c. In the FABMS spectra of the sample solutions used, the fragmentation pattern did not change when matrices of different proton affinities were used for the same analyte. This observation appears to contradict the G.C.M. at a first glance because gaseous media are involved in the CI experiment and in the FAB cavity. An important difference between these two situations is the high density and the high temperature of the FAB cavity. The temperature of the

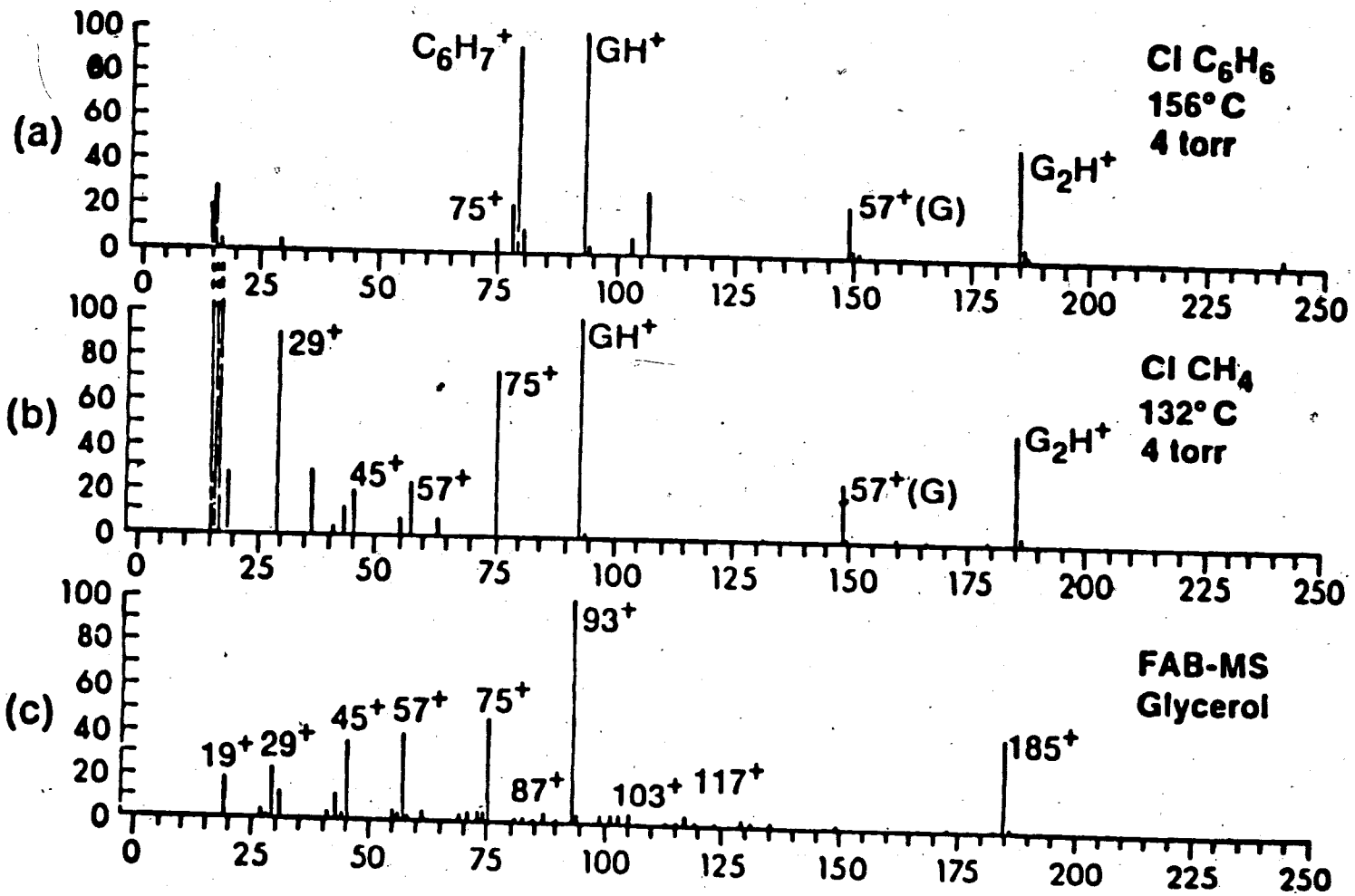

FIGURE

(9a) Chemical ionization mass spectrum of glycerol in 4 torr of methane with 2% (mole) benzene.

(9b) Chemical ionization mass spectrum of glycerol in 4 torr of methane.

(9c) FAB spectrum of neat glycerol.

cavity could be assumed to be similar in all cases. Due to the high density of the cavity, a protonated analyte molecule produced by the proton transfer from a given protonated matrix molecule will undergo several rapid, non-reactive collisions with nearby molecules. These collisions will ultimately lead to a thermalized ion. The internal energy of this thermalized ion becomes essentially independent of the exothermicity of the protonation reaction, i.e., in FAB the ions will leave the surface with similar distribution of internal energy that is characteristic of the "temperature" of the cavity.

4.4 Stability of the protonated dimers and their intensities in FABMS

One common feature in most FABMS spectra is the appearance of proton bound dimers, of the matrix molecules and sometimes of the analyte molecules. The intensities of the proton bound dimers observed in the FAB spectra of the compounds such as glycerol, butanetriol and diethanolamine, etc., are given in Table II. The equilibrium constants for the formation of dimers at 500 K represented by the following equation are also given in Table II. These equilibrium constants were obtained by J. Sunner from this laboratory using a pulsed high pressure ion source mass spectrometer (31).

$$MH^+ + M \longrightarrow M_2H^+ \qquad (7)$$

$$K_{eq} = (M_2H^+)/(MH^+) \times P_M \qquad (8)$$

As can be seen from the values given in Table 2, the intensity ratio of M_2H^+ to MH^+ increases with the value of Keq. This would mean that the thermodynamic stability of the dimer relative to the monomer has increased with Keq. The only exception to the above trend is the octylaniline. Although the Keq for octylaniline is greater than that for DEA, the observed FAB dimer/monomer intensity ratio of the aniline is much less than that of DEA. A possible explanation of this observation would be occurrence of decomposition of the dimer clusters of the aniline during the time of flight in the mass spectrometer. At high temperatures one would expect large molecules to have internal energies greater than the dissociation energies of the clusters (33). Therefore, these clusters may undergo rapid unimolecular dissociations during the time of flight in the mass spectrometer.

Table 2. Stabilities of proton bound matrix dimers

	$Keq^{a}/torr^{-1}$ at 500 K	$\frac{I(M_2H^+)^{b}}{I(MH^+)}$
NOBA	?	0.13
Glycerol	1 200	0.33
Butanetriol	1 200	0.22
Octylaniline	100	0.07
Diethanolamine	4.6	0.12
Triethanolamine	0.8[c]	0.01

a) Keq for reaction: $MH^+ + M = M_2H^+$, standard state 1 atm.

b) Intensity ratio between the proton bound dimer and the protonated matrix molecule as observed in FAB spectra of the pure matrix.

c) Estimated.

CHAPTER V

5.0 Secondary ion currents of preionized liquids in FAB

In the precursor model of FAB, the desorption of secondary ions is assumed to be due largely to direct momentum transfer from the fast atoms to the preformed (i.e., existing) ions in the liquid sample. The preformed ions thus are expelled into the vacuum. Assuming this to be true one would expect that the total intensity of the secondary ions or the total ion current (TIC) will depend on the concentration of the "preformed ions" in the sample. If the concentration of the preformed ions is increased by the addition of salts or acids to the liquid matrix, one would expect an increase in the TIC. In order to examine whether this is the case, measurements of the TIC from FAB were performed. Surprisingly, even though TIC measurements are relatively straight forward, such measurements have not been reported in the literature. The total ion currents of glycerol containing increasing concentrations of soluble salts and acids were measured. The corresponding mass analyzed FAB spectra were also recorded. The experimental procedures for the TIC measurements are described in the experimental part.

The results of the TIC measurements of the alkali chloride (MCl) solutions are given in Table 3 and the plot of mole percent alkali chloride in glycerol versus the TIC alkali chloride/TIC glycerol is given in Figure 10.

Table 3: Total ion currents of alkali chlorides in glycerol

(a) LiCl in glycerol:

Mole % LiCl	TIC LiCl in glycerol/TIC glycerol
0.2	0.91
0.5	0.92
1	0.90
2	0.93
4	1.10
8	1.05

(b) KCl in glycerol:

Mole % KCL	TIC KCl in glycerol/TIC glycerol
0.2	1.03
0.5	0.95
1	0.91
2	0.97
4	1.01
8	0.99

Table 3: Continued.

(c) RbCl in glycerol:

Mole % RbCl	TIC RbCl in glycerol/TIC glycerol
0.1	0.92
0.5	0.86
1	0.84
2	0.75
4	0.84
8	0.82

(d) NaCl in glycerol:

Mole % NaCl	TIC NaCl in glycerol/TIC glycerol
0.2	0.97
0.5	0.94
1	0.91
2	0.95
4	0.88
8	0.86

FIGURE 10

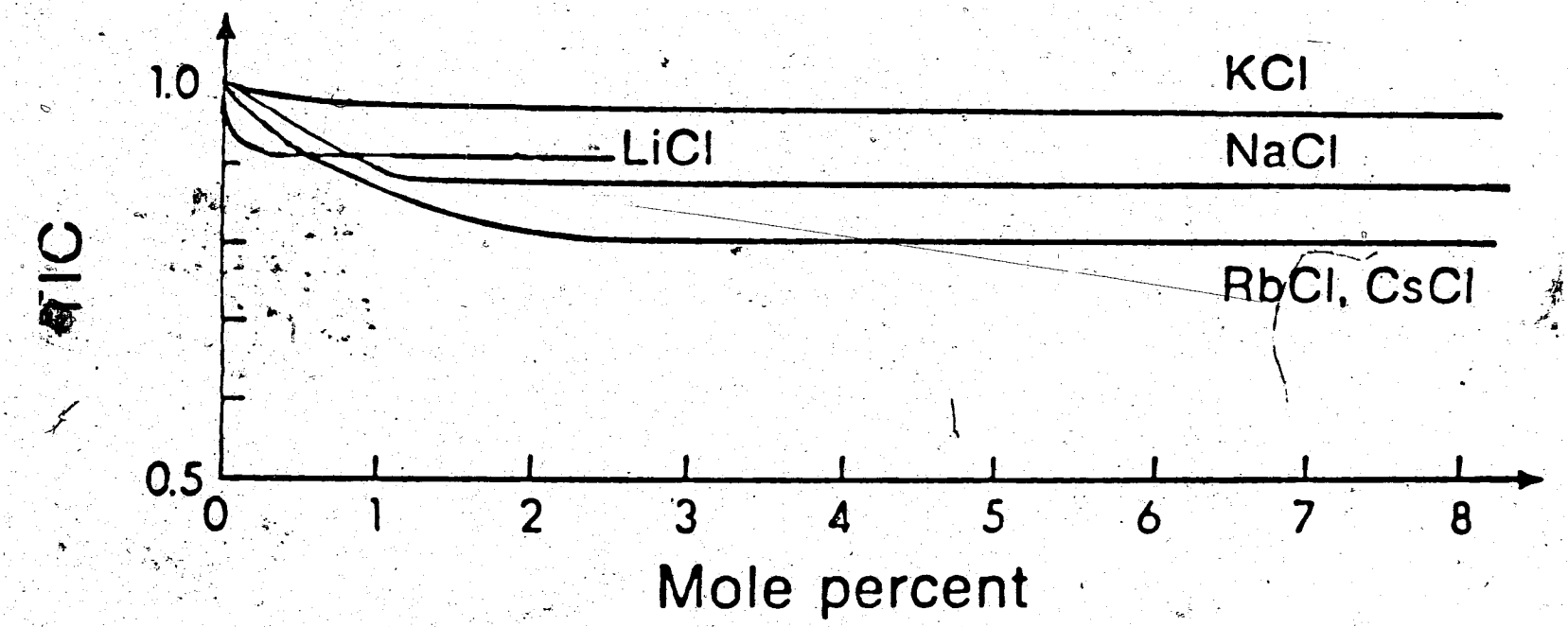

TIC from glycerol solutions of alkali chlorides.

It is apparent from these figures that the TIC does not increase with the added concentration of the salts, i.e., there is no increase in the TIC with the concentration of the preformed ions in the sample solution. In fact, a decrease in the TIC is observed initially in all cases. A notable feature in this figure is the decrease in TIC for all the salts occurring below 0.5 mole percent. Another observation that can be made from these plots is the order of the initial decrease in the TIC which is K < Li < Na < Rb. After the initial decrease, the total ion current remains relatively constant with further increase of the salt concentration.

5.1 The influence of alkali chlorides on FAB spectra

Typical FAB spectra of 1 mole percent solutions of LiCl, NaCl, and KCl in glycerol are shown in Figures 11-13, respectively. In the spectra of glycerol solutions of the alkali chlorides we have assigned the ions to three groups:

(i) The metal ion (M^+) and the mixed clusters of the metal and glycerol molecules $(M^+)_n\ (Cl^-)_{n-1}\ (Gly)_m$, and $(M^+)_2\ (Gly\text{-}H)^-\ (Gly)_m$ where Gly = glycerol.

(ii) The protonated ion of glycerol ($GlyH^+$), its major fragment ions (m/e = 75^+, 45^+, 57^+) and the protonated glycerol dimers and trimers.

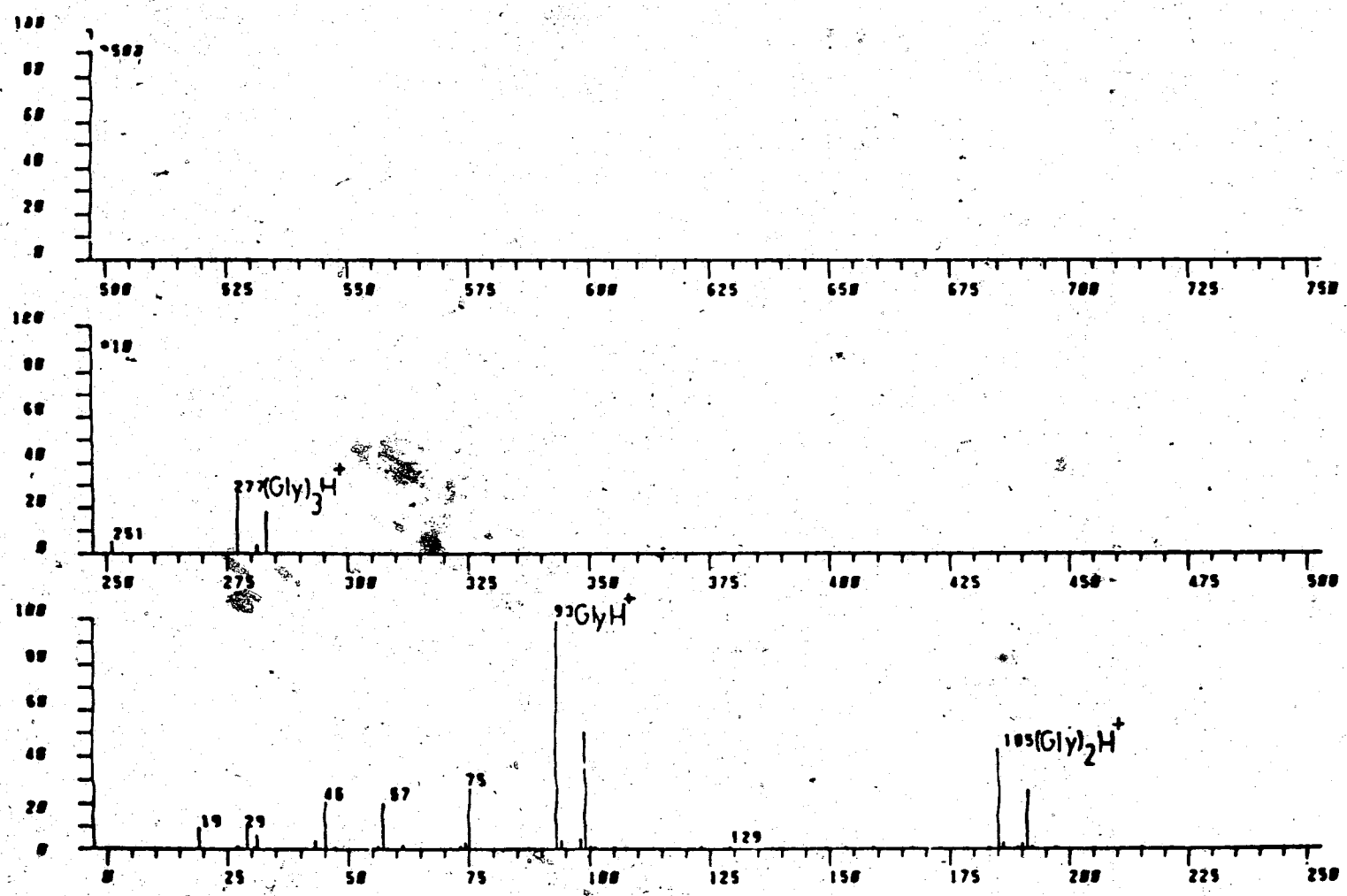

Figure 11 FAB spectrum of 1 mole percent LiCl in glycerol.

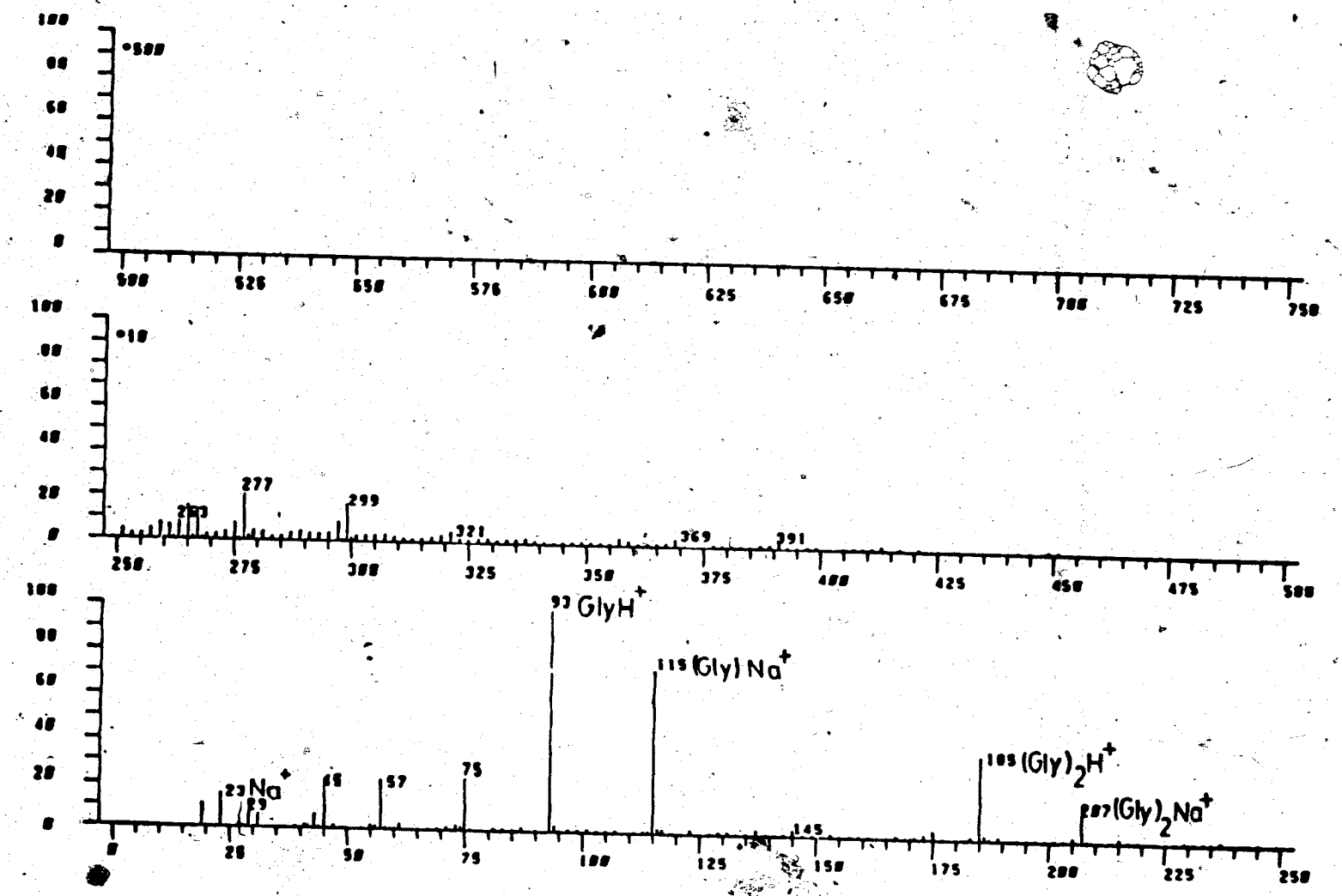

Figure 12 FAB spectrum of 1 mole percent NaCl in glycerol.

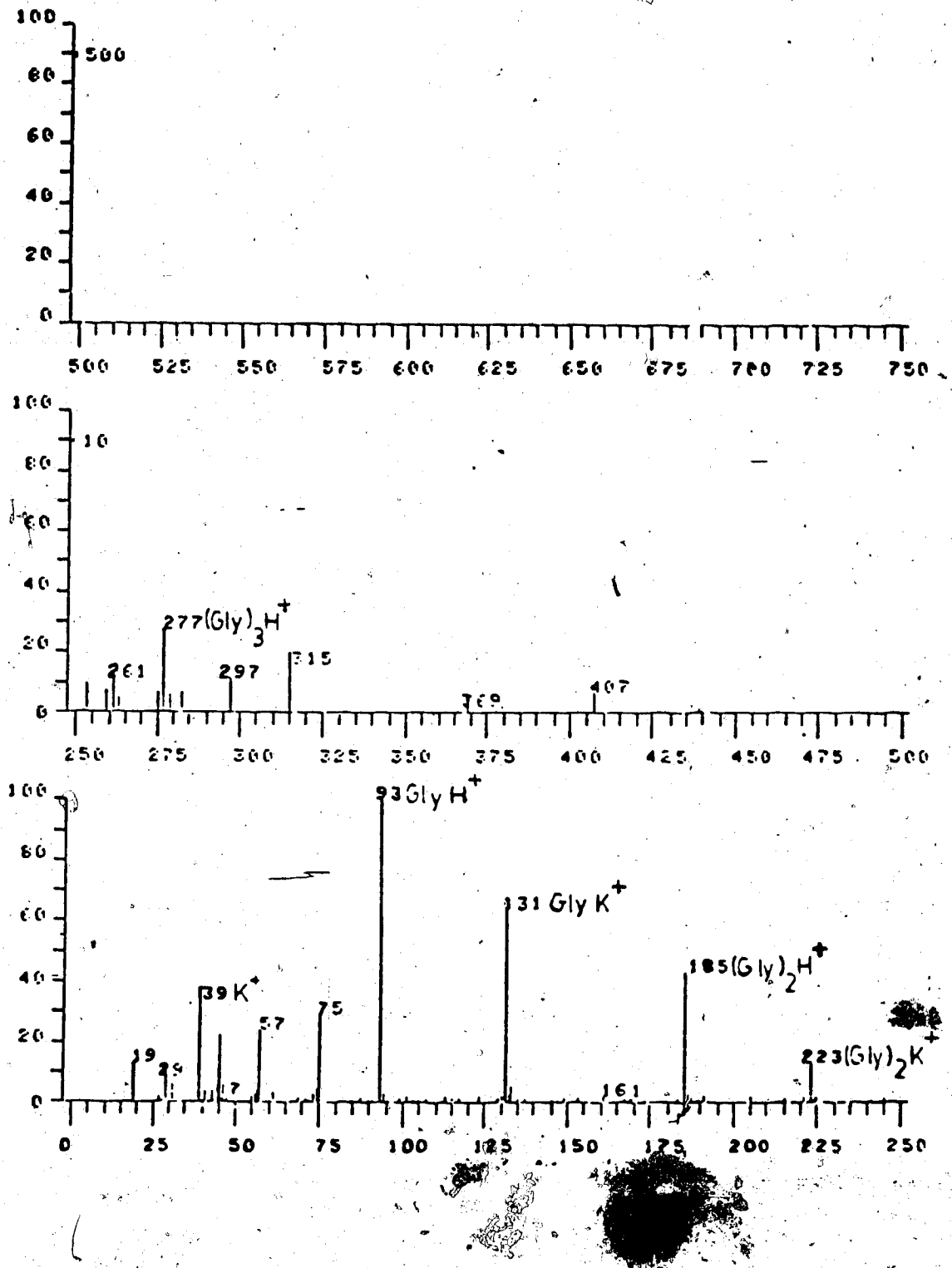

Figure 13 FAB spectrum of 1 mole percent of KCl in glycerol.

(iii) The background peak "noise" extends over the complete mass range.

Table 4 shows the intensities of these three groups of ions for KCl in glycerol and Figure 14 gives a plot of the groups intensities (as a percent of TIC) versus the mole percent of KCl in glycerol.

Table 4: FABMS peak intensities of alkali chlorides

Mole %	K^+ Containing Peaks	Glycerol Containing Peaks	Background Ions
0	0	56	44
0.1	4	68	28
0.2	6	67	27
0.5	13	60	27
1.0	25	47	28
2.0	38	31	31
4.0	57	19	24
8.0	72	6	22

One observes a rapid increase in the intensit[illegible] alkali containing ions with increased concentrati[illegible] KCl and a corresponding decrease in the glycerol [illegible]ining ions. A notable feature in this figure is that at very low concentrations of KCl (< 0.5 mole percent), there is a

FIGURE 14

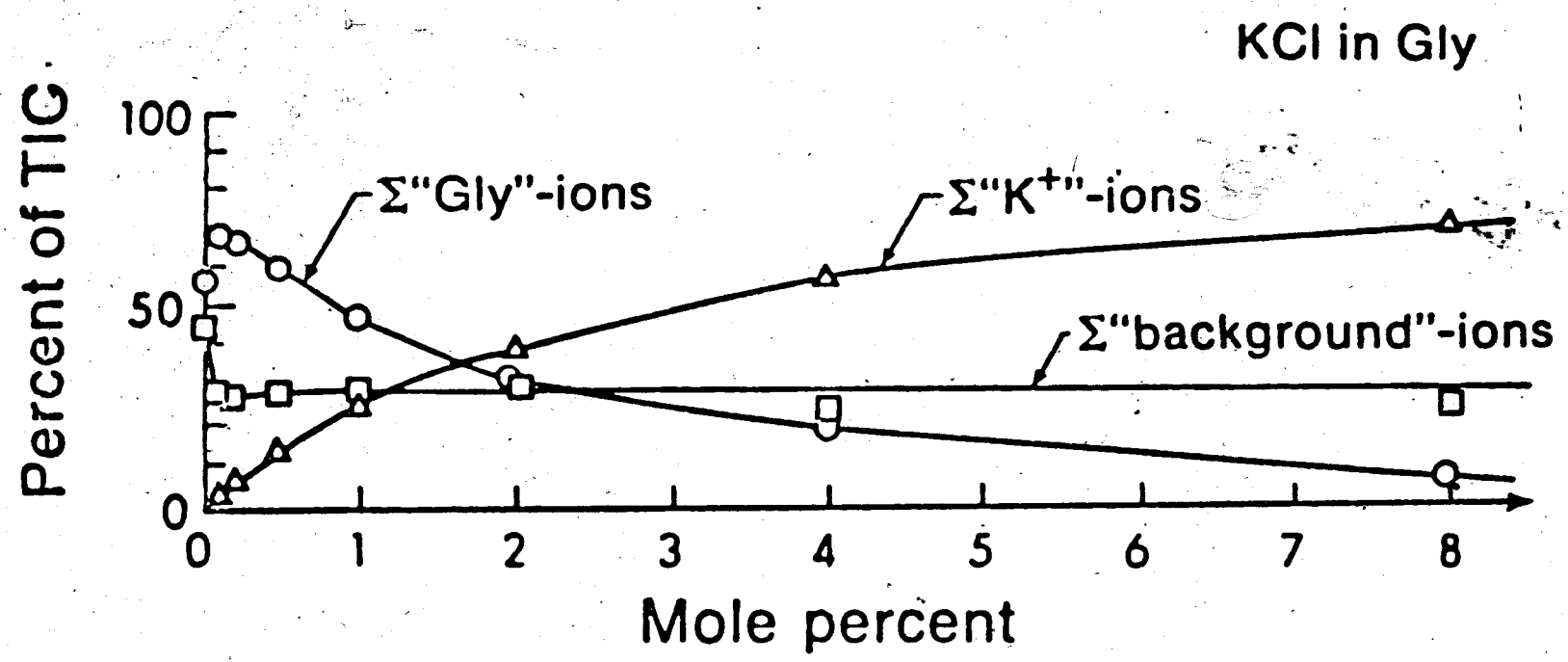

Sum of intensities of all K^+ containing ions, sum of intensities of the main glycerol ions and sum of intensities of background ions.

marked increased in the intensity of the main glycerol ions and a corresponding drop in the background peaks. It appears that traces of the salt tend to "clean-up" the glycerol spectrum. One could also observe a drop in the intensities of main fragment ions of glycerol relative to $GlyH^+$, at very low concentrations of alkali chlorides in glycerol.

A plot of intensity of the major glycerol fragments/ intensity of $GlyH^+$ versus mole percent of KCl in glycerol (Table 5 and Figure 15) illustrates this point in more detail.

Table 5: Fragment to monomer intensity ratios of glycerol in KCl/glycerol solutions.

	Intensity of glycerol fragments
Mole % KCl in glycerol	Intensity of $GlyH^+$
0	0.79
0.1	0.71
0.2	0.65
0.5	0.67
1.0	0.75
2.0	0.75
4.0	1.10
8.0	2.10

FIGURE 15

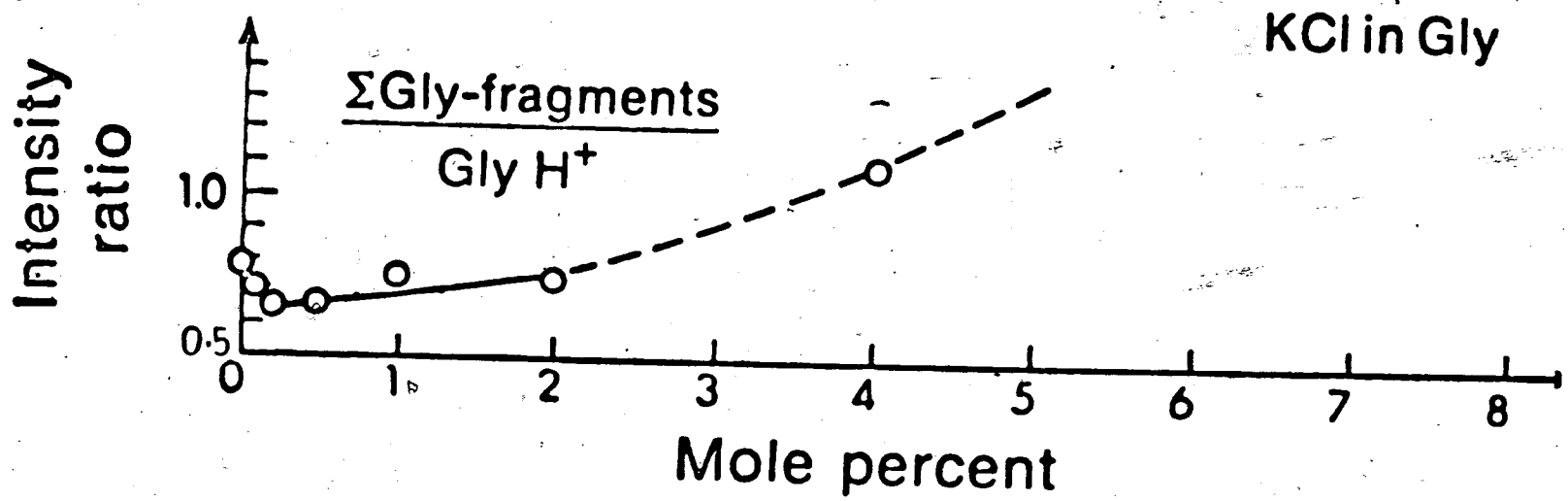

Ratio of sum of intensities of the main glycerol fragments 75^+, 57^+ and 45^+, to the intensity of the protonated glycerol ions.

The above curve shows an improvement from a 0.79 fragments to monomer ratio for neat glycerol to a 0.65 fragments to monomer ratio at a KCl concentration of 0.2 mole percent.

The observed glycerol dimer to monomer intensity ratio is plotted against the mole percent KCl in glycerol (Table 6 and Figure 16). After an initial dimer to monomer ratio increase at very low concentration of KCl, a gradual decrease of the ratio is observed with the increasing concentration of KCl.

Table 6: Dimer to monomer intensity ratios of glycerol in KCl/glycerol solutions.

Mole % KCl	$(Gly)_2 H^+/GlyH^+$
0	0.43
0.1	0.46
0.2	0.52
0.5	0.50
1.0	0.43
2.0	0.32
4.0	0.22

It is noteworthy that the increase in the total glycerol containing peaks, the decrease in the fragment

FIGURE 16

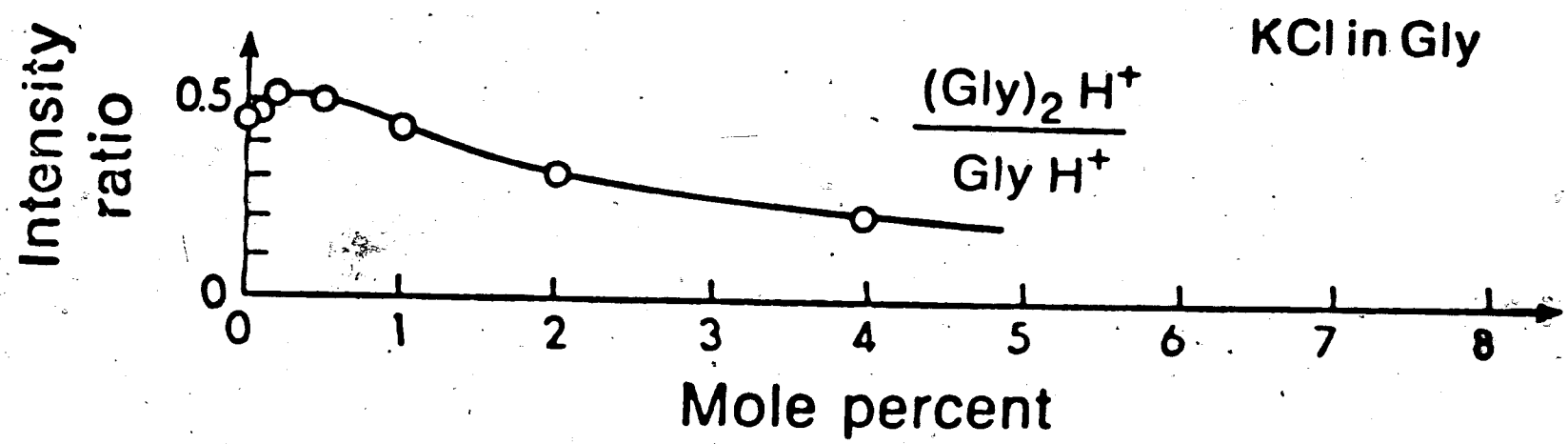

Ratio of protonated glycerol dimer to the protonated monomer.

ratio of glycerol and the increase in the dimer to monomer ratio of glycerol occur approximately in the same concentration range of KCl in glycerol (0.1 - 0.5 mole %). The plots for the other alkali chlorides were similar.

The apparent increase in the degree of fragmentation of the glycerol and the decrease in the $Gly_2H^+/GlyH^+$ ratio as the concentrations of MCl increases from 0.5 mole percent to 8 mole percent can be explained as a consequence of the gas expulsion process from the cavity. We can assume that the gas expelled early is much hotter than the gas expelled later because the "latter" gas will be cooled by the adiabatic expansion in the cavity. Therefore, it is reasonable to assume that the fragmentation is more extensive in the "early" gas. In the case of neat glycerol, the bottom gas will contain more of the $GlyH^+$ and the Gly_2H^+. When we add alkali chlorides, $GlyH^+$ formed in the bottom gas will have sufficient time to undergo ion molecule reactions with the alkali chlorides resulting in M^+ and $GlyM^+$. This considerably reduces the concentration of the $GlyH^+$. Thus, an apparent increase in the degree of fragmentation relative to the monomer ($GlyH^+$) is seen in the FAB spectra.

A preference factor (P.F.) for alkali ions over the matrix ions can be defined as follows:

$$P.F. = \frac{\text{Total intensity of peaks containing alkali ions}}{\text{Total intensity of matrix ion peaks}} \times \frac{\text{Moles matrix}}{\text{Moles alkali ions}}$$

The relation between P.F. and mole % KCl in glycerol is shown in Table 7 and Figure 17. The plots for the other alkali ions were similar.

Table 7: Preference factors of K^+ over glycerol ions in KCl/glycerol solutions

Mole % KCl in glycerol	P.F.
0.1	41.2
0.2	39.7
0.5	46.2
1.0	49.0
2.0	59.1
4.0	72.3
8.0	129.6

The preference factors obtained for the alkali ions ($\approx$ 40 - 100) are in the same range as the P.F.'s obtained for the neutral compounds discussed previously. However, a major difference between the bases and the alkali chlorides is that the P.F.'s for the alkali chlorides increase with the concentration of the analyte. The

FIGURE 17

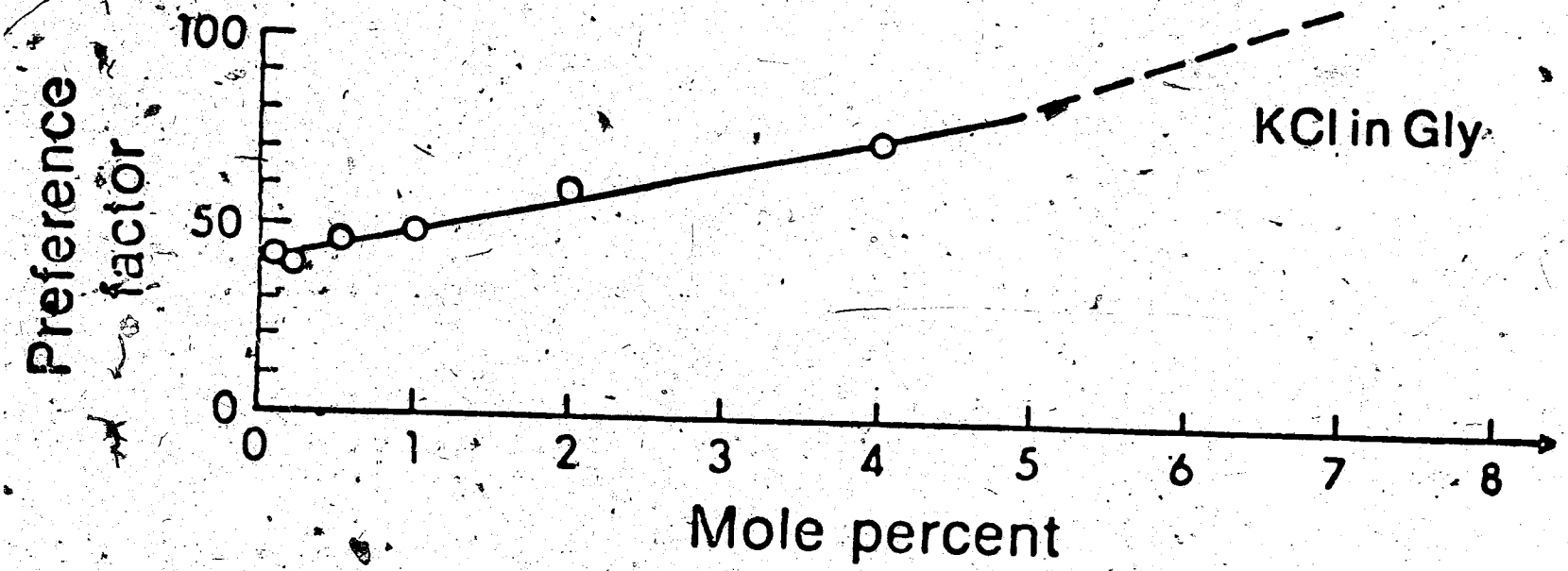

Preference factors for K^+ containing ions over the main glycerol ions.

reasons for such a difference are discussed in Section 5.6.

The P.F.'s for 1 mole % solutions of alkali chlorides in glycerol and in TEA are given in Table 8 and Figure 18.

Table 8: Preference factors of alkali ions in glycerol and in TEA

(a) 1% MCl in glycerol:

MCl	P.F.
LiCl	36
NaCl	54
KCl	49
RbCl	45

(b) 1% MCl in TEA:

MCl	P.F.
LiCl	23
NaCl	26
KCl	26
RbCl	22

It appears from these plots that the preference factors are influenced not only by the concentration of the analyte, but also by the chemical environment of the analyte. The P.F.'s for the alkali chlorides are higher

FIGURE 18

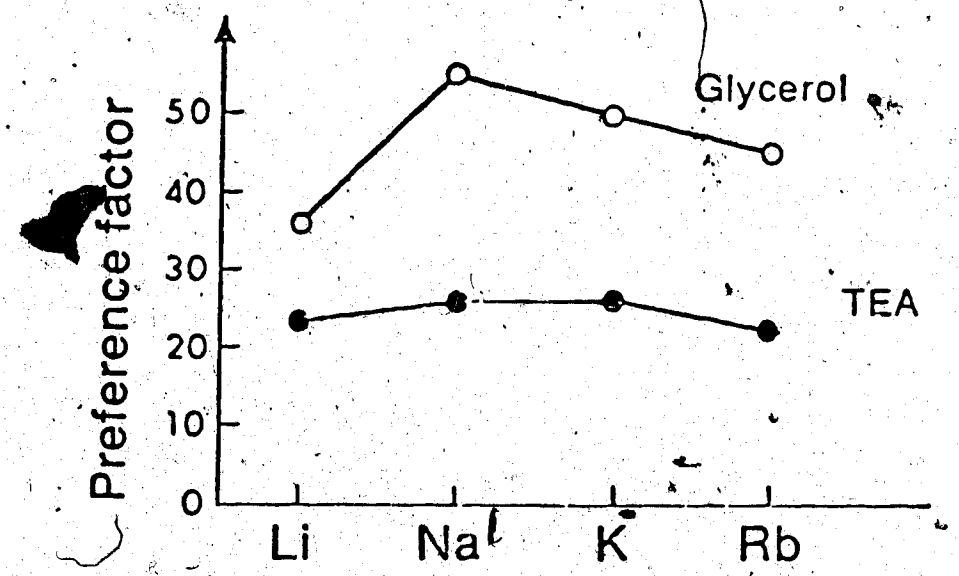

Preference factors for alkali containing ions over matrix ions for 1 mole percent solutions of alkali chlorides in glycerol and in triethanolamine

in glycerol than in TEA. Since the proton affinity of TEA is greater than that of glycerol, the P.F.'s obtained for the alkali chlorides in TEA and glycerol appear to be in accordance with a gas phase collision model rather than with a precursor model. If the ionization occurs according to a precursor model, one would expect similar P.F.'s for the same analyte concentration regardless of the matrix because the intensity of a particular ion depends on the concentration of the pre-existing ions in solution.

5.2 The influence of HCl on FAB spectra and TIC

The change in the TIC upon the addition of concentrated HCl in glycerol is shown in Table 9 and Figure 19. It is apparent that the overall change in the TIC is small. It should be noted that when concentrated HCl is added to the glycerol, a certain amount of H_2O is also introduced. To determine whether H_2O had any effect on the TIC, experiments were performed with glycerol/H_2O mixtures. No significant changes in TIC were observed of these mixtures with respect to the pure glycerol samples.

Table 9: Total ion currents of Gly/HCl solutions

Mole % HCl in glycerol	TIC Gly/HCl/TIC glycerol
0.0	1
0.1	0.86
0.2	0.77
0.5	0.84
1.0	0.89
2.0	0.97
4.0	0.94
8.0	1.03
16	1.06

Although there is no overall change in the TIC, a significant dip in the TIC was observed at very low concentrations of HCl in glycerol ($\approx$ 0.1 mole %). This is quite similar to what was observed with the alkali chlorides in glycerol. But in this instance, the TIC increases with the concentration of HCl, and remains relatively constant at high concentrations of HCl. In the case of the alkali chlorides, no increase in the TIC was observed after the initial depression. Table 10 and Figure 20 show the variation of the total intensities (as percentage of TIC) of the main glycerol peaks and the intensities of the pseudomolecular glycerol ion ($GlyH^+$) with the concentration of the HCl in glycerol. Table 11 and Figure 21 show the variation of the intensity ratio between the main fragments

FIGURE 19

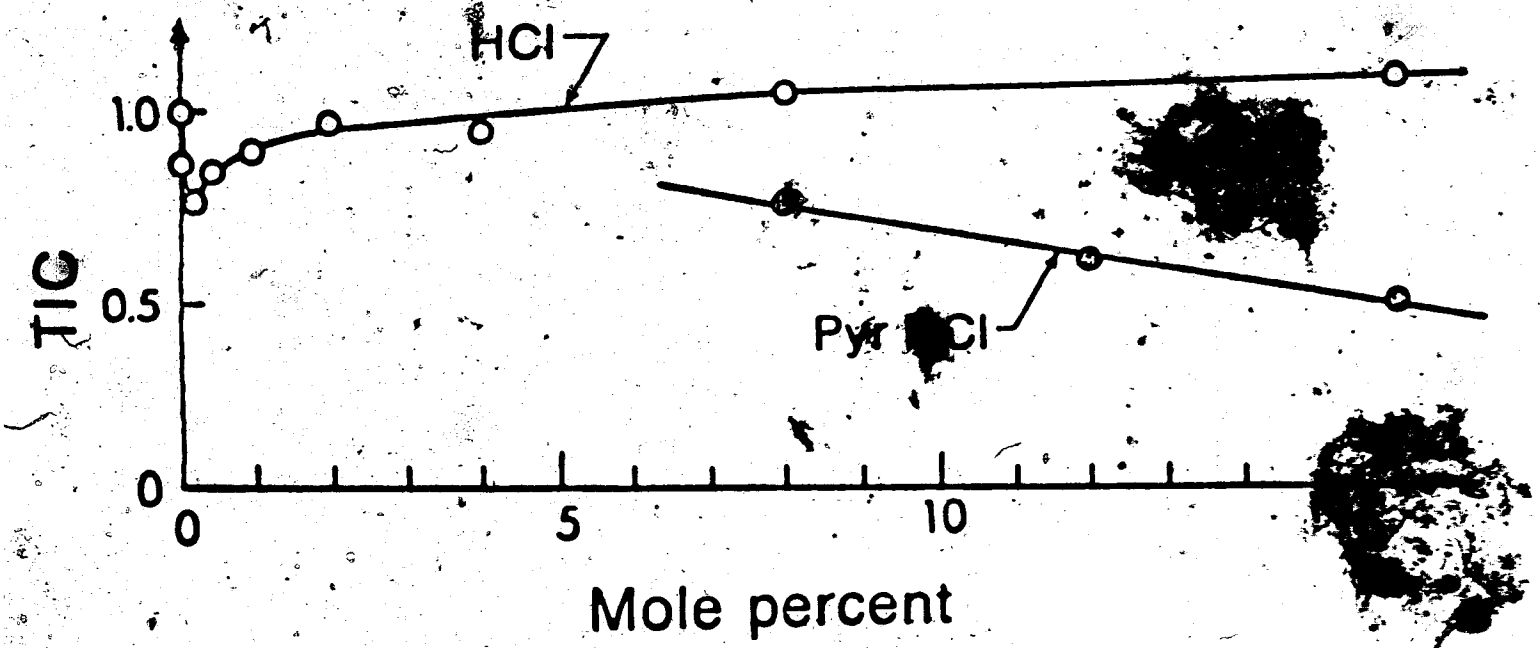

TIC of glycerol with concentrated HCl and TIC for glycerol with pyridinium hydrochloride.

Table 10a: Intensities of the main glycerol ions in HCl/Gly solutions

Mole % HCL	Intensity of main glycerol ions as a % of TIC
0	60.1
0.2	43.5
1.0	39.4
2.0	31.2
4.0	29.4
8.0	28.4
16.0	32.2

Table 10b: Intensities of the $GlyH^+$ in Gly/HCl solutions

Mole % HCL	Intensity of $GlyH^+$ as a % of TIC
0	27.1
0.2	18.6
1.0	16.3
2.0	10.8
4.0	10.4
8.0	8.8
16.0	10.3

FIGURE 20

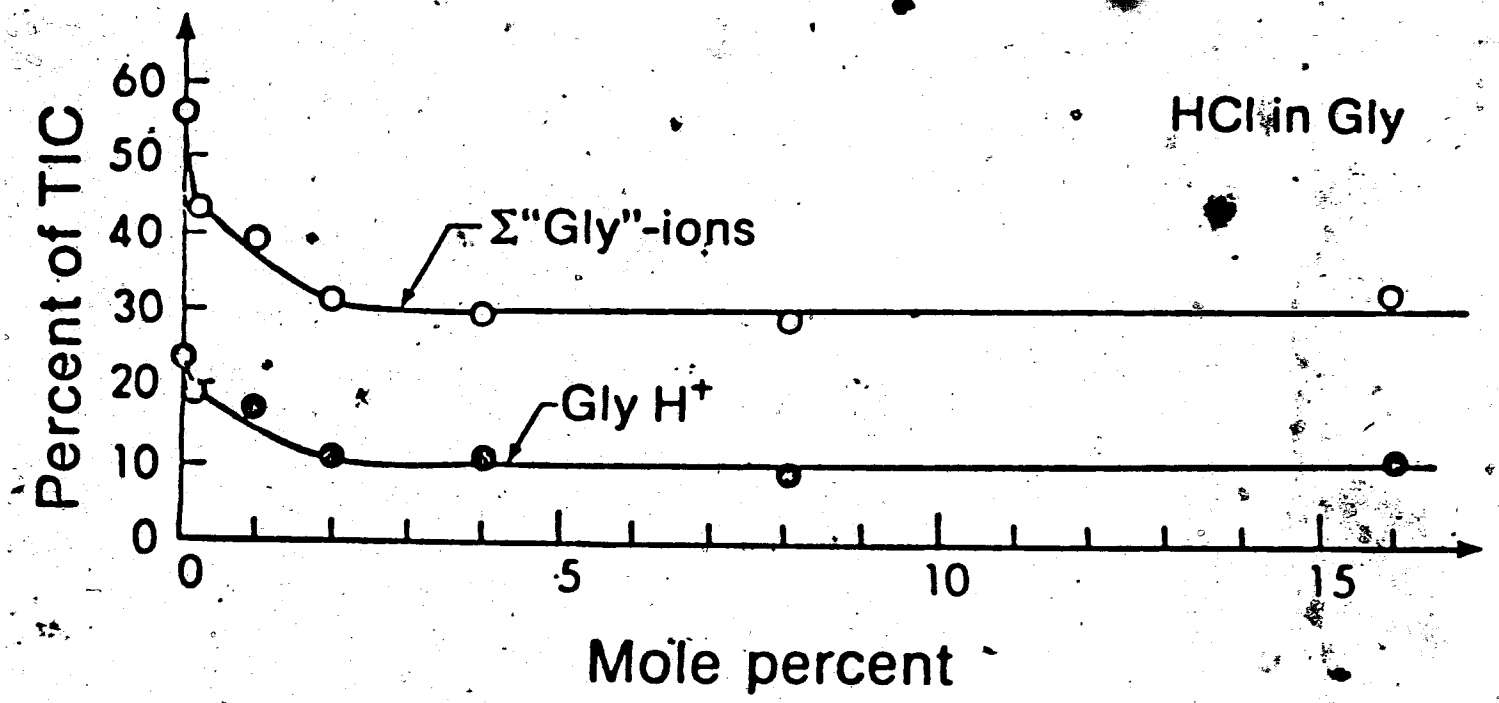

Sum of intensities of main glycerol ions and intensities of protonated glycerol ions.

Table 11: Intensity ratios of the main fragments of glycerol to the intensity of $GlyH^+$

Mole % HCL	Intensity of main fragments of glycerol / Intensity of $GlyH^+$
0	0.74
0.2	0.96
1.0	1.07
2.0	1.44
4.0	1.48
8.0	1.93
16.0	1.76

Table 12: Intensity ratios of dimer to monomer peaks of glycerol in HCl/Gly solutions

Mole % HCL	Intensity dimer/Intensity monomer
0	0.45
0.2	0.37
1.0	0.33
2.0	0.40
4.0	0.35
8.0	0.30
16.0	0.37

FIGURE 21

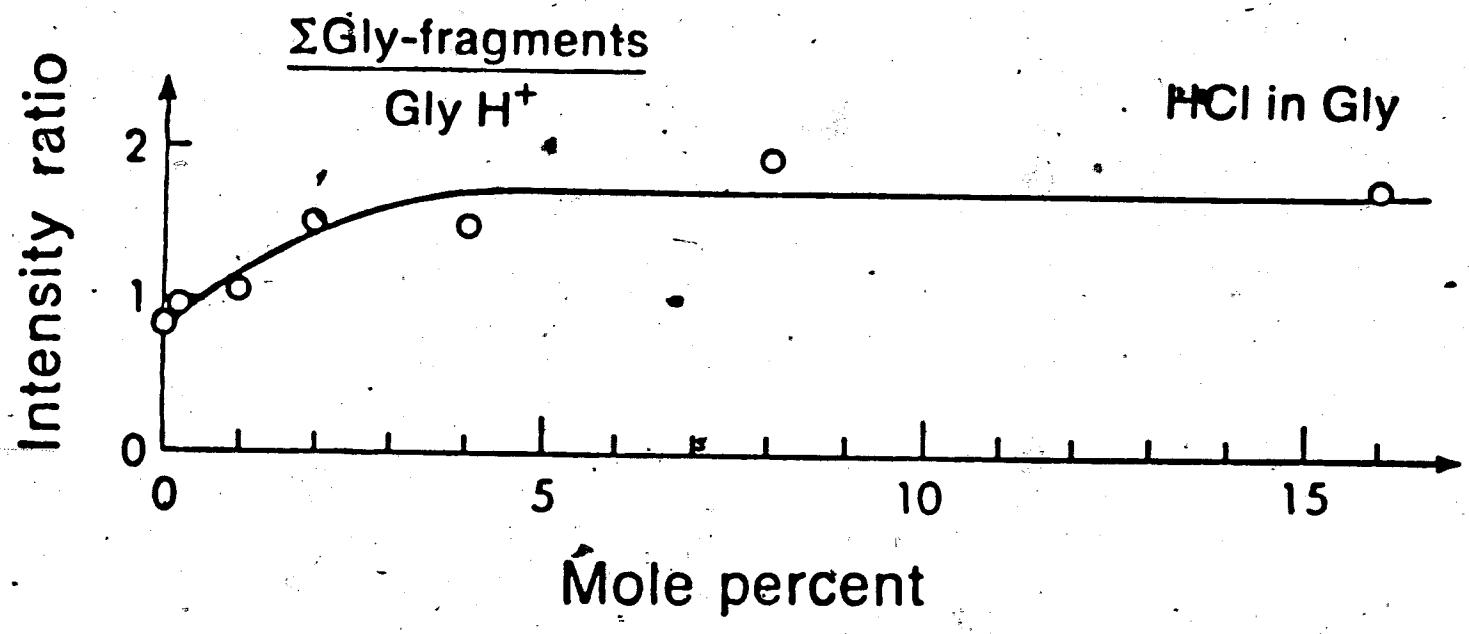

Ratio of sum of intensities of the main glycerol fragments, 75^+, 57^+ and 45^+, to the intensity of the protonated glycerol ions.

of glycerol and $GlyH^+$ with the concentration of HCl in glycerol. The dimer to monomer ratio of glycerol is plotted against the concentration of HCl in glycerol (Table 12 and Figure 22).

On inspection of Figure 20, one could observe a decrease in the intensity of $GlyH^+$ it low concentrations of HCl by about a factor of 2, [illegible]sult, a corresponding decrease in the intensity of the main glycerol peaks in the same concentration range could be seen. As in the case of the TIC measurements, the intensities of the $GlyH^+$ and the main glycerol ions remain constant at higher concentrations of HCl. Since the TIC is relatively constant during the experiments, except for the initial decrease at very low concentrations, it was concluded that the addition of HCl to glycerol decreases the intensity of the main glycerol ions and increases the background ion intensity by a similar amount. The ratio of the intensity of the fragment ions of glycerol to the $GlyH^+$ increases at the same low concentration range mentioned previously (Figure [illegible]). This increase in the fragment to monomer ratio coincides with a decrease in the dimer to monomer ratio at very low concentrations (Figure 22). The trends observed in TIC measurements and peak intensities in glycerol/HCl mixtures at low analyte concentrations appear

FIGURE 22

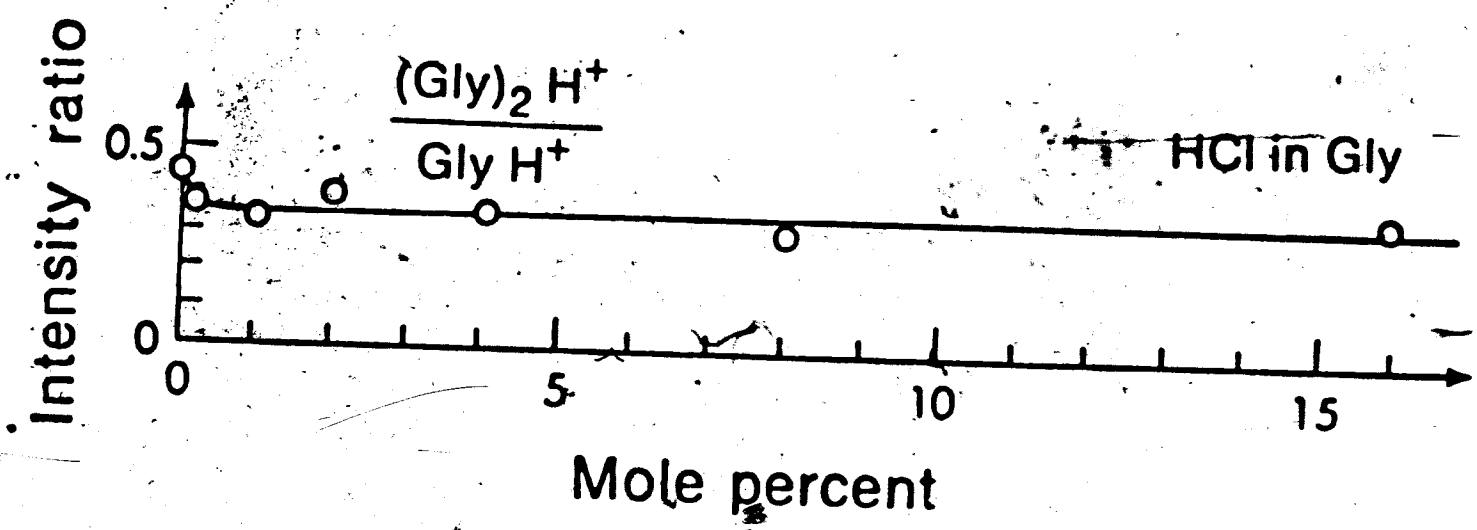

Ratio of the protonated glycerol dimer to the protonated monomer.

to be in the reverse order to what was observed for alkali chloride/glycerol mixtures at the same concentration levels.

When the TIC measurements were performed with pyridinium hydrochloride/glycerol mixtures, a continuous decrease in the TIC was observed with increasing concentration of the hydrochloride (Figure 9). This is again contrary to what was observed with the alkali chloride/glycerol mixtures. Figure 23 depicts the variation of TIC's for different mixtures of diethanolamine (DEA) and diethanolamine hydrochloride (DEAHCl) (Table 13).

Table 13: Variation of TIC of DEAHCl/DEA solutions

Mole % of DEAHCl in DEA	TIC DEAHCl/TIC DEA
0	1.0
25	0.76
50	0.46
75	0.41
100	0.46

DEAHCl in the pure form is a liquid and hence can be used as a FAB matrix. Here again a decrease in the TIC's is observed at low salt concentrations in a manner similar to the pyridinium hydrochloride/glycerol mixtures.

FIGURE 23

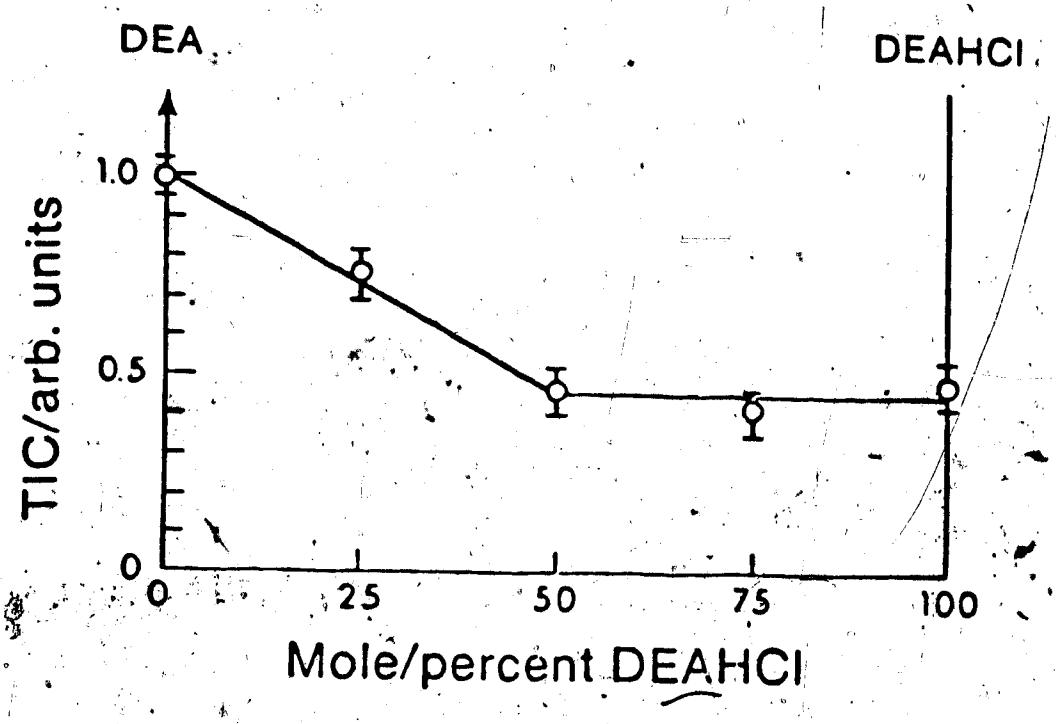

TIC for mixtures of diethanolamine and diethanolamine hydrochlorides.

The above results clearly indicate that for all cases studied so far, the presence of preformed ions in the liquid matrix, whether they are protonated molecules or alkali ions, does not increase the total ion current upon the atom bombardment. In all cases a depression of the TIC is observed initially at low concentrations of the analytes and a subsequent stabilization of the current occurs at higher concentrations, except in the cases of DEAHCl and pyridinium hydrochloride where the TIC decreased at high concentrations. When one considers the FABMS spectra of the sample mixtures discussed so far, major changes in the intensities of certain ions are observed, with increasing analyte concentrations. For instance, trace amounts of alkali ions in glycerol tend to "clean up" the glycerol spectrum by increasing the signal intensity of the main glycerol peaks and decreasing the background peaks. The results that have been presented so far are not consistent with a precursor model but instead suggest that ion molecule reactions are important in determining the nature of the FAB ions. It will be shown in the next section how these results can be explained with the gas phase collision model (G.C.M.).

5.3 Total ion currents in gas collision model

The G.C. model, as described in the introduction, implies the occurrence of a collision cascade in the liquid sample due to the impact of the fast atom. When the atoms of the sample are hit head on by the high energy primary atoms, the sample atoms will be torn away from the rest of the molecule and undergo collisions with neighbouring sample molecules. This sequence of events will eventually lead to the formation of a cavity which contains a high density, high temperature gas consisting of sample molecules and ionic fragments. At this stage it is possible for ion molecule reactions to take place within the cavity to produce pseudomolecular ions and cluster ions. The initial ions are produced by the collisions of the fast atom beam with neutral matrix and analyte molecules. Such an ionization process must be responsible for the observation of FAB spectra of neutral matrices and analytes.

The sequence of reactions leading to the protonated matrix (glycerol) ions may be represented as follows:

$$\vec{A} + Gly \longrightarrow Pi^{+} \qquad (9)$$

$$Pi^{+} + F \longrightarrow Si^{+} \qquad (10)$$

$$Si^{+} + Gly \longrightarrow GlyH^{+} \qquad (11)$$

$\vec{A}$ = bombarding atom, Pi^+ = a primary ion, F = neutral fragment, Si^+ = secondary ion.

The addition of salts to the liquid sample may be expected to increase the degree of ionization described above if we assume that the ions of the electrolyte are "desorbed" into the gas. As a result, the TIC would be expected to increase with the concentration of the salt in the matrix. The results we have presented contradict this assumption. Therefore, one could conclude that the total ion current or the number of ions in the gas are determined not only by the initial ionization process caused by the atom bombardment, but also by the nature of the desorption process. In the desorption process, extensive positive-negative ion recombination may be occurring. The gas phase energetics of alkali halides show that ion pair recombination in the gas phase is energetically favourable. For example, if one considers the energy stability diagram of NaCl (Figure 24), it can be seen that the formation of the ion pair $Na^+Cl^-(g)$ from $Na^+(g)$ and $Cl^-(g)$ is a highly exothermic reaction (ΔH = -450 kJ/mole).

5.4 Evidence for recombination reactions

5.4.1 Estimate of ions produced per FAB particle

Let us assume that the total emission of secondary ions extends over an area of about $(\pi/2)r^2$ of a sphere with

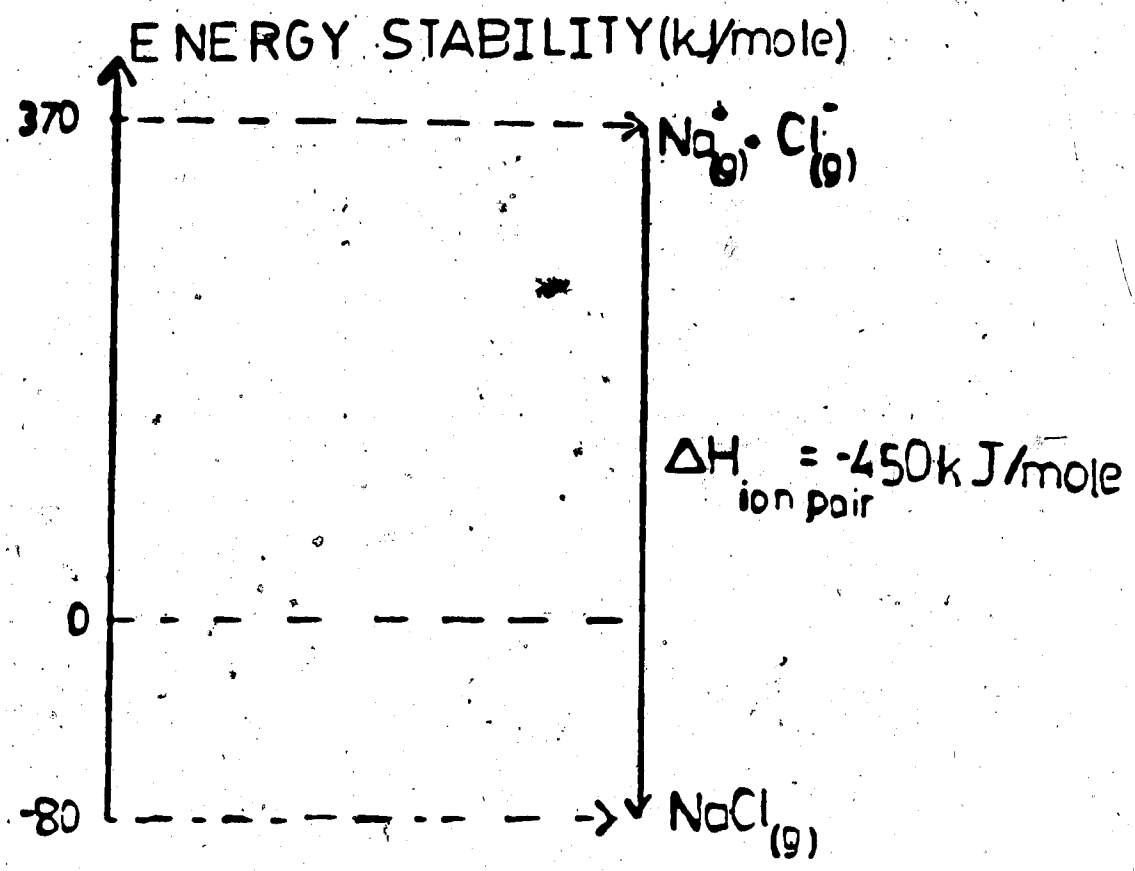

Energy Stability Diagram of NaCl in the Gas Phase

Figure 24

radius (r), where r is the distance from the probe tip to the ion exit slit. The area of the ion exit slit is approximately 0.1 cm^2 and r = 1 cm. Therefore, the ratio of the area of the slit to the total emission is given by 0.1 x 2/3.14 x 1 = 0.05., i.e., approximately only 1/20 of the total number of secondary ions produced would actually get through the exit slit. The total ion currents of the alkali chloride solutions in glycerol were in the range of 10^{-8} amp. Since the charge of an ion is 6 x 10^{-19} coulombs, the current of 10^{-8} amp would correspond to $10^{-8}/6 \times 10^{-19}$

= 10^{10} ions/second. Since only 1/20 of the total number of ions get through the slit, the ions actually produced would be 2 x 10^{11} ions/second. The FAB gun fast particle emission has been measured (34) to be about 10^{13} particles per second. These numbers imply that only 0.01 ions per incident particle escape from the target into the vacuum as a result of the fast atom bombardment of the sample.

5.4.2 Ions from liquid matrix and analyte

The total number of matrix molecules expected to be desorbed by an atom impact can be estimated as follows. The energy of the fast atoms produced by the FAB gun has been measured to be about 6 keV (34). This corresponds to about 138,000 kcal per mole. The heat of vapourization of glycerol is 18 kcal per mole. This would mean that as a result of the atom impact, a maximum of 7,000 molecules of the matrix are desorbed. Since some of the energy will be dissipated in other modes such as heat transfer to matrix and fragmentation of matrix molecules, the expected number of glycerol molecules evaporated should be much smaller. Alternatively, the number of desorbed molcules can also be calculated from the size of the cavity produced by the impact. Magee has reported (25) that the depth of a cavity formed by the atom impact is about 40 Å. If we assume

that this cavity is in the shape of a cube with sides of 40 Å the corresponding volume will be 64 x 10^{-21} cm^3. The density of glycerol is 1.2 g/cm^3, and with the known molecular weight, 92 g/mole, the number of molecules of glycerol contained in the cavity is found to be about 600. For convenience we can assume that some 1000 molecules of glycerol are desorbed as a result of one atom impact.

In the experiments we performed, we have used 5 mole percent solutions of electrolyte in glycerol. This would lead to the production of 50 ions if one assumes that all the electrolyte ions contained amongst the 1,000 glycerol molecules become desorbed. In the case of the neat neutral matrix such as glycerol, the number of ions expected from the total number of glycerol molecules described can be calculated utilizing the ionization cross-sections of some fast atoms quoted by Michl (27). The ionization cross-sections of Ar projectiles impacting on gaseous H with 5 keV energy is about 10^{-16} cm^2. For Xe with about 8 keV energy we could assume the ionization cross-section to be about 10^{-15} cm^2. Therefore, the number of ions produced in an area of 10^{-15} cm^2 and at a depth of 40 Å as a result of the atom impact is about 3. However, the collision cascade contains many secondary fast atoms produced from the glycerol molecules and the fastest of

these will also produce some ionization. Therefore, some 10 or more ions per impacting particle in neat glycerol could be produced. This indicates that ion recombination reactions must be occurring since much fewer ions leave the target, than are produced by the impact. Recombination is a second order reaction. The rate equation for a second order reaction is:

$$C = 1/[kt + (1/C_o)] \qquad (12)$$

c = concentration at time t, C_o = initial concentration, t = time during which recombination occurs. Recombination will terminate as gas expands into vacuum.

It was calculated on page 85 that there are 0.01 ions observed per impact, and an initial production of about 10 ions per impact expected for glycerol. Substituting these numbers in equation (12), one obtains a value for kt which equals 100.

$$0.01 = 1/[kt + (1/10)]$$

$$kt \simeq 100$$

Using this value of kt in equation (12) one finds that an increase of C_o from 10 to 50, due to the presence of preformed ions will lead to a negligible increase of the final ion concentration, i.e., from C = 0.01 to C = 0.0101.

As a result of the second order kinetics of the recombination, there is no appreciable increase in the final ion concentration for changes of the initial concentration by

factors of four. Our experimental results show that the addition of electrolytes to the matrix leaves the TIC relatively constant, which con[illegible] occurrence of an extensive recombination process.

5.5 Thermodynamic feasibility of analyte ion formation from ion pairs

The following reactions may be assumed to occur in the gas phase in FABMS experiments:

$$GlyH^+ + MX \longrightarrow M^+ + XH + Gly \quad (13)$$

$$GlyH^+ + MX \longrightarrow M^+(Gly) + XH \quad (14)$$

Using the tabulated standard entropy values (35) for M, XH, MX at 300 K and the value for the entropy change on protonation for glycerol calculated by J. Sunner (31), I have estimated an average value for the entropy change for reaction 13 (ΔS°_{13}) for all alkali ions to be about 45 cal/K mole. The enthalpy change for reaction 13 is $\Delta H^\circ_{13} = PA\ (Gly) + \Delta H^\circ_f(XH) - \Delta H^\circ_f(H^+) - \Delta H^\circ_f(MX) + \Delta H^\circ_f(M^+)$. Using the P.A. value for glycerol 209 kcal/mole (31), together with the tabulated standard heats of formation (35), one could then calculate ΔH°_{13} for all the alkali ions.

McNeal has reported (36) that the temperature of the cavity in FABMS is about 1,000 K. Substituting the above

values in the following equation: $\Delta G = \Delta H - T\Delta S$ (15), ΔG^{o}_{13} is calculated to be at 1,000 K as -10, -32, -46, -48 and -53 kcal/mole for M = Li, Na, K, Rb and Cs, respectively.

As there are no major structural changes between the products and reactants in reaction (14), and also since there is no net creation of molecules, ΔS^{o}_{14} can be assumed to be zero. ΔH^{o}_{14} has been estimated by J. Sunner (37). From the values of ΔH^{o}_{14} and ΔS^{o}_{14} one can estimate the value of ΔG^{o}_{14} at 1,000 K. The values obtained for the alkali ions are between -30 to -40 kcal per mole. Comparing the values of ΔG^{o}_{13} given above with ΔG^{o}_{14} = 35 kcal/mole, one finds that ΔG^{o}_{14} is larger for Li and Na than ΔG^{o}_{13}, which means that for these ions reaction 14 will dominate over reaction 13. This is in agreement with the intensity ratios observed in FABMS spectra for $M^{+}(Gly)/M^{+}$ given below in table 14. Similarly in the case of K and Rb, reaction 13 appears to dominate over 14.

In Figure 25 the log of the intensity ratio $M^{+}(Gly)/M^{+}$ for the different alkali ions is plotted against ΔG^{o}_{16}(38) for the model reaction $M^{+} + 2H_2O \longrightarrow M^{+}(H_2O)_2$ (16).

Table 14: Correlation between intensity ratio of $M^+(Gly)/M^+$ and $-\Delta G^o_{16}$

Intensity (M^+Gly)/Intensity M^+		$-\Delta G^o_{16}$ kcal/mole
27	Li^+	47
5.0	Na^+	31
1.69	K^+	20
1.15	Rb^+	17

The comparison between reactions 16 and $M^+ + Gly \rightarrow M^+(Gly)$ (17) is valid for the following reasons: Due to the simple electrostatic nature of the interaction between the alkali ions and neutral molecules, the bond energy of $M^+(Gly)$ and of $M^+(H_2O)_2$ should change proportionally as the alkali ion is changed. The entropy and free energy changes should obey similar proportional relationships. At equilibrium equation 18 will hold:

$$\ln [(M^+(Gly)/M^+)] \propto \Delta G^o_{16}/RT \qquad (18)$$

The linear relationship found in Figure 25 does not necessarily imply that reaction 17 is at equilibrium, though an approach to equilibrium may occur.

5.6 Preference factors of alkali chloride solutions

It was mentioned in Section 4.2 that I had experimentally observed that the preference factors of the

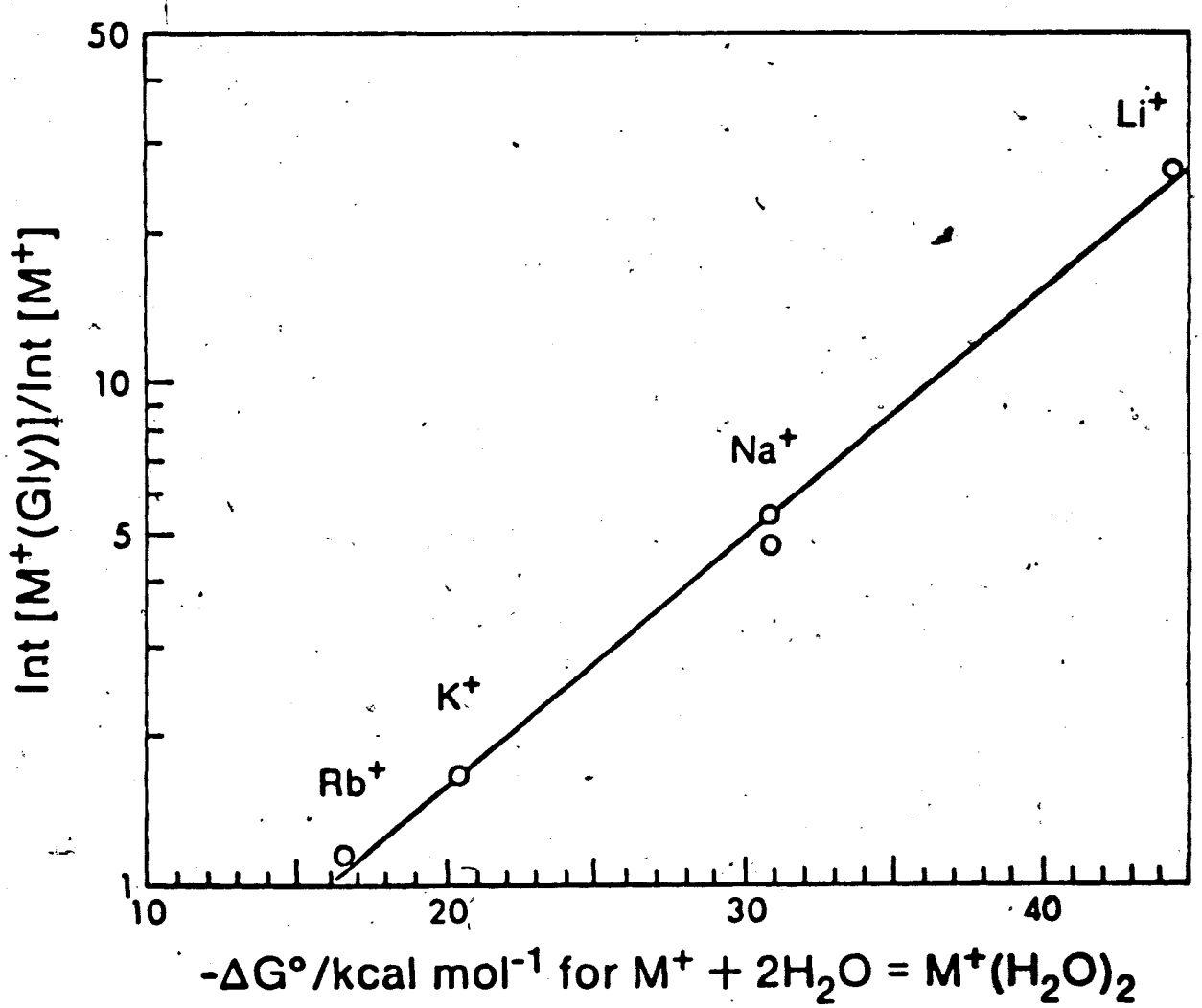

Figure 25 Correlation between the FAB intensity ratio at 1 mole percent MCl: $M^+(Gly)/M^+$ and $-\Delta G^o$ at 300 K for the clustering reaction $M^+ + 2H_2O \longrightarrow M^+(H_2O)_2$[16] for M = Li^+, Na^+, K^+ and Rb^+.

neutral compounds did not change significantly when the concentrations of these compounds were increased from 0.1 to 10 mole percent. As there are no preformed ions in the matrix in this case, all ions must originate from the collision cascade resulting from the atom bombardment. The preference found for the analyte is explained as a consequence of the following protonation reaction (19) leading to the analyte ions.

$$GlyH^+ + Analyte \longrightarrow Gly + (Analyte)H^+ \qquad (19)$$

In the case of alkali chlorides it was observed that at low concentrations the P.F.'s for alkali containing ions are of the same magnitude, 35 to 55, as for the neutral analytes. This again can be explained by the ion molecule reactions (13) and (14). However, in contrast to the neutral analytes, the P.F.'s for the alkali ions increase quite significantly with increasing concentration of the alkali chlorides (Figure 17). This increase can be explained as follows: In addition to the alkali containing ions formed by the ion molecule reactions, there will be a residual amount of alkali ions (M^+) which did not undergo the recombination reactions. When the concentrations of the alkali chlorides increase, the amount of residual alkali ions will also increase. Therefore, the P.F.'s will increase with the concentration of the alkali ions. According to this picture, some of the ions observed

in the FAB spectra, at least the alkali ions, are indeed formed by the vapourization of preformed ions.

CHAPTER VI

C O N C L U S I O N

An attempt has been made to explain the ion formation in fast atom bombardment mass spectrometry. In the first part of this thesis I have presented a study of the influence of gas phase basicities of analytes and matrices on FAB spectra. It was found that pseudomolecular ions, MH^+, of high basicity compounds had higher intensities in the spectra than ions of low basicity compounds. It was concluded that a number of collisions occur in the gas phase after the impact of the atom but prior to the entrance of the ions into the vacuum. Some of these collisions result in proton transfer.

In the second part of the thesis I have demonstrated the importance of gas phase energetics to the extent of cation formation in FAB. It was also shown how gas phase ion pair formation can be utilized to explain TIC results of electrolyte samples in FABMS.

Future Experiments

The results I obtained indicate that competition for protons by means of gas phase proton transfer reactions

occurs. Since there is a rough correlation between gas phase basicities and aqueous basicities, it can be argued that the competition may actually occur in the liquid matrix. In order to clarify this, experiments should be performed to study the competition for protons between specially chosen analyte pairs. One of the compounds in the pair should have the higher gas phase basicity, but the other should be more basic in the liquid matrix.

References

1. Barber, M.; and Brodoli, R.S., Sedgewick, R.D. J. Chem. Soc., Chem. Commun. 1981, 325.

2. Barber, M. in "Soft Ionization Biological Mass Spectrometry", Morris, H.R. (Ed.), Heyden, London, 1981.

3. Kerr, R.A. Science 1982, 216, 163.

4. Busch, K.L.; Cooks, R.G. Science 1982, 218, 247.

5. Benninghoven, A. Int. J. Mass Spectrom. Ion Phys. 1983, 46, 459.

6. Aberth, W.; Burlingame, A. Anal. Chem. 1982, 54, 2029.

7. Benninghoven, A. in "Ion Formation from Organic Solids", Benninghoven, A. (Ed.), Springer-Verlag, 1983 Chapter 3.1.

8. Fenselau, C. in "Ion Formation from Organic Solids", Benninghoven, A. (Ed.), Springer-Verlag, 1983 Chapter 3.2.

9. Martin, S.; Biemann, K. Anal. Chem. 1982, 54, 2362.

10. Morris, H.R.; Haskins, J. Int. J. Mass Spectrom. Ion Phys. 1983, 46, 363.

11. Rinehart, K. Science 1982, 218, 254.

12. McNeal, C.J. Anal. Chem. 1982, 54, 43A.

13. Barber, M.; Sedgewick, S. Biomed. Mass Spectrom. 1982, 9, 11.

14. Barber, M.; Bordoli, S. Org. Mass Spectrom. 1981, 16, 256.

15. Barber, M.; Bordoli, S. Anal. Chem. 1982, 54, 645A.

16. Gower, J.L. Matrix Compounds for FAB, An Interim Review, Chemotherapeutic Research Centre, Surrey, England.

17. Przybylski, M.; Fresenius Z. Anal. Chem. 1983, 315, 402.

18. Puzo, G.; Prome, J.C. Org. Mass Spectrom. 1984, 19, 448.

19. Dallinga, J.W.; Nibbering, N. Org. Mass Spectrom. 1984, 19, 10.

20. Dell, A.; Ballou, C. Biomed. Mass Spectrom. 1983, 10, 50.

21. Lehman, W.D.; Kong, W. Biomed. Mass Spectrom. 1984, 11, 217.

22. Meli, J.; Seibl, J. Org. Mass Spectrom. 1984, 19, 581.

23. Suzuki, M.; Harada, K. Org. Mass Spectrom. 1982, 17, 386.

24. Williams, D.H.; Taylor, C. J. Am. Chem. Soc. 1981, 103, 5700.

25. Magee, C.W. Int. J. Mass Spectrom. Ion Phys. 1983, 46, 459.

26. Cooks, R.G. Int. J. Mass Spectrom. Ion Phys. 1983, 53, 111.

27. Michl, J. Int. J. Mass Spectrom. Ion Phys. 1983, 53, 255.

28. Jonkman, H.; Michl, J. J. Am. Chem. Soc. 1981, 103, 733.

29. Orth, R.; Michl, J. J. Am. Chem. Soc. 1982, 104, 1834.

30. Hogg, A. Int. J. Mass Spectrom, Ion Phys. 1983, 49, 25.

31. Sunner, J.; Kulatunga, R.; Kebarle, P. Anal. Chem. in Press, 1986.

32. Perrin, D. "Dissociation Constants of Organic Bases in Aqueous Solution", Butterworths, London, 1965.

33. Sunner, J.; Kebarle, P. J. Phys. Chem. 1981, 85, 327.

34. Hogg, A. Int. J. Mass Spectrom. Ion Phys. in Press, 1986.

35. Wagman, D. J. Phys. Chem. Ref. Data 1982, 11, Suppl. 2.

36. McNeal, C. Anal. Chem. 1982, 54, 43A.

37. Sunner, J.; Kulatunga, R.; Kebarle, P. Anal. Chem. in Press, 1986.

38. Kebarle, P. Ann. Rev. Phys. Chem. 1977, 28, 445.